Iranian Journal of Mathematical Chemistry, Vol. 7, No. 2, October 2016, pp. 113 – 153 **IJMC**

Type–Itemized Enumeration of RS–Stereoisomers of Octahedral Complexes

SHINSAKU FUJITA

Shonan Institute of Chemoinformatics and Mathematical Chemistry, Kaneko 479-7

Ooimachi, Ashigara-Kami-Gun, Kanagawa-Ken, 258-0019 Japan

Correspondence should be addressed to SHINSAKU FUJITA (EMAIL: shinsaku_fujita@nifty.com)

Received 16 November 2015; Accepted 24 November 2015

ACADEMIC EDITOR: ALI REZA ASHRAFI

ABSTRACT Stereoisograms of octahedral complexes are classified into five types (type I–type V) under the action of the corresponding *RS*-stereoisomeric group. Their enumeration is accomplished in a type-itemized fashion, where Fujita's proligand method developed originally for combinatorial enumeration under point groups (S. Fujita, *Theor. Chem. Acc.*, 113, 73–79 (2005)) is extended to meet the requirement of Fujita's stereoisogram approach. The cycle index with chirality fittingness (CI-CF) of the point group O_h is modulated by taking account of the CI-CF for calculating type-V quadruplets contained in stereoisograms. The modulated CI-CF is combined with a CI-CF of the maximum chiral point group (O), a CI-CF of the maximum *RS*-permutation group, a CI-CF of the maximum ligand-reflection group, and a CI-CF of the *RS*-stereoisomeric group, so as to generate CI-CFs for evaluating type-I to type-V quadruplets. By introducing ligand-inventory functions into the CI-CFs, the numbers of quadruplets of octahedral complexes are obtained and shown in tabular forms. Several stereoisograms for typical complexes are depicted. Their configuration indices and *C/A*-descriptors are discussed on the basis of Fujita's stereoisogram approach.

KEYWORDS enumeration • stereoisogram • octahedral complex • *RS*–stereoisomeric group.

1. INTRODUCTION

Fujita's stereoisogram approach has been developed by defining *RS-stereoisomeric groups* as algebraic formulations [1, 2] and *stereoisograms* as their diagrammatic expressions [3, 4, 5]. Diagrammatically speaking, the vertical direction of a stereoisogram is concerned with the chiral aspect for supporting Le Bel's way (dissymmetry, chirality) [6, 7] and the horizontal direction of a stereoisogram is concerned with the *RS*-stereogenic aspect for

supporting van't Hoff's way (asymmetry, stereogenicity) [8, 9]. Thereby, these two ways have been integrated to reach Aufheben, so that the theoretical foundations of modern stereochemistry and the terminology of stereochemical nomenclature (e.g., the Cahn-In gold-Prelog system [10, 11] and the *pro-R/pro-S* system [12, 13, 14]) have been thoroughly revised, as discussed in recent articles [15, 16, 17, 18].

A quadruplet of *RS*-stereoisomers contained in a stereoisogram can be regarded as an equivalence class under the action of an *RS*-stereoisomeric group. This means that the number of inequivalent quadruplets can be combinatorially enumerated by extending Fujita's unit-subducedcycle- index (USCI) approach [19, 20] to meet the requirement of Fujita's stereoisogram approach, if the data of the *RS*-stereoisomeric group (e.g., mark tables, inverse mark tables, and subduction tables) are available. According to this guideline, symmetry-itemized enumerations of quadruplets of *RS*-stereoisomers have been reported by starting from a tetrahedral skeleton [21, 22], an allene skeleton [23, 24], and an oxirane skeleton [25, 26, 27]. It is to be noted, however, that mark tables, inverse mark tables, and subduction tables for the *RS*-stereoisomeric groups have been obtained by rather tedious procedures even in the enumerations based on the above-mentioned skeletons of ligancy 4.

As for the action of point groups, derivatives to be counted can be classified into two categories, i.e., chiral and achiral derivatives. According to this classification, chirality-itemized enumeration for aiming at itemization into chiral and achiral derivatives has been accomplished by using Fujita's proligand method [28], which has been developed as a simpler method for gross enumeration than those supported by Fujita's USCI approach for symmetry-itemized enumeration [19, 20]. Note that Fujita's proligand method applied to such chirality-itemized enumeration does not requires mark tables, inverse mark tables, and subduction tables, which are not always available.

In a similar way to chirality-itemized enumeration under the action of point groups, it is desirable to investigate type-itemized enumeration of inequivalent quadruplets under the action of an *RS*-stereoisomeric group, because such quadruplets of *RS*-stereoisomers as represented by stereoisograms have been proven to be categorized into five types (type I to type V) [2]. Type-itemized enumerations of quadruplets of *RS*-stereoisomers based on inclusion-exclusion procedures [29, 30] and on more systematic procedures [31, 32] have been reported by using tetrahedral and allene derivatives as probes of ligancy 4.

Because the more systematic procedures [31, 32] are expected to have wide applicability, they should be examined extensively by being applied to more complicated derivatives. The present article is devoted to the application of one of the procedures (using cycle indices with chirality fittingness modulated by type-V quadruplets [32]) to octahedral complexes of ligancy 6.

2. *RS*-STEREOISOMERIC GROUPS FOR OCTAHEDRAL COMPLEXES

2.1. ALGEBRAIC FORMULATION OF *RS*-STEREOISOMERIC GROUPS

Although the algebraic formulation of an *RS*-stereoisomeric group $O_{h\tilde{l}\hat{I}}$ for characterizing an octahedral skeleton 1 has been described in a previous report [33], a minimal set of data should be cited here for the sake of convenience.

By starting from the point group O_h for characterizing an octahedral skeleton 1, the *RS*- stereoisomeric group $O_{h\tilde{l}\hat{I}}$ is represented by the following coset decomposition:

$$O_{h\tilde{l}\hat{I}} = O + O\,i + O\,\tilde{l} + O\,\hat{I} \qquad (1)$$

where the group O is the maximal chiral subgroup of the point group of O_h, the first representative *I* (omitted for the sake of simplicity) is an identity operation, the second representative *i* is an inversion operation, the third representative $\tilde{l}$ is an *RS*-permutation operation, and the fourth representative $\hat{I}$ is a ligand-reflection operation.

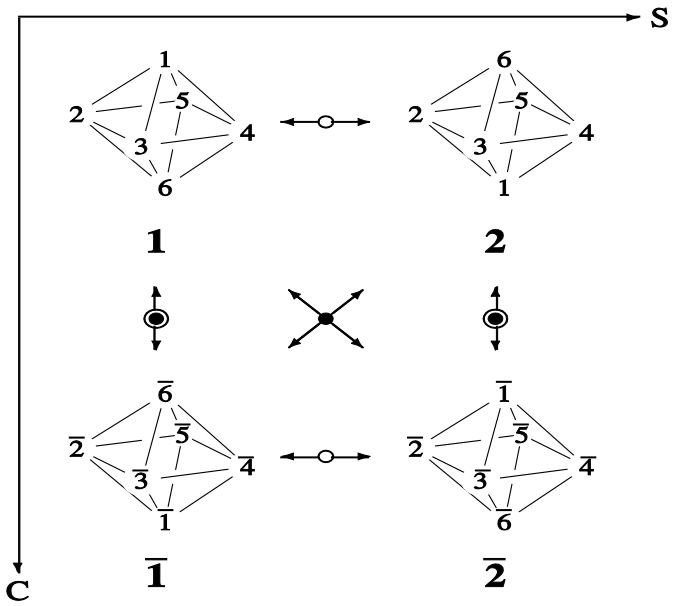

Figure 1. Elementary stereoisogram of an octahedral skeleton [33].

The 96 elements of the *RS*-stereoisomeric group $O_{h\tilde{l}\hat{I}}$ (Eq. 1) are collected in Figure 2. According to the coset decomposition represented by Eq. 1, they are categorized into four parts, as denoted by large gray letters (A, B, C, and D):

1. The upper left part denoted by a gray letter A in Figure 2 corresponds to the coset O (= O*I*). When the representative of this coset is selected to the identity element *I* which is assigned to the representative skeleton 1, the other operations contained in the coset O(= O*I*) generate respective homomers of 1. The operations collected in the upper left part (A) are called *rotations*.
2. The lower left part denoted by a gray letter B in Figure 2 corresponds to the coset O*i*. When the representative of this coset is selected to a reflection $\sigma_{h(1)}$ in place of *i*, a mirror-image skeleton $\bar{1}$ is generated as a representative (Figure 1). The other operations contained in the coset O*i* (= O$\sigma_{h(1)}$) generate respective homomers of $\bar{1}$. The operations collected in the lower left part (B) are called *reflections*, which connote rotoreflections (e.g., $S_{4(1)}$) and an inversion (*i*) in addition to mirror-image operations.
3. The upper right part denoted by a gray letter C in Figure 2 corresponds to the coset $O\tilde{I}$. When the representative of this coset is selected to an *RS*-permutation in place of $\tilde{I}$, an *RS*-permuted skeleton 2 is generated as a representative (Figure 1). The other operations contained in the coset $O\tilde{I}$ (= $O\tilde{\sigma}_{h(1)}$) generate respective homomers of 2. The operations collected in the upper right part (C) are called *RS-permutations*.
4. The lower right part denoted by a gray letter D in Figure 2 corresponds to the coset $O\hat{I}$. When the representative of this coset is selected to a ligand reflection $\hat{I}$, an *RS*-ligand reflected skeleton $\bar{2}$ is generated as a representative (Figure 1). The other operations contained in the coset $O\hat{I}$ generate respective homomers of $\bar{2}$. The operations collected in the lower right part (D) are called *ligand reflections*.

The *RS*-stereoisomeric group $O_{h\tilde{I}\hat{I}}$ collected in Figure 2 has 96 elements (order 96) and contains the following subgroups of order 48.

The maximum point group (A + B):

$$O_h = O+Oi \tag{2}$$

The maximum *RS*-permutation group (A + C):

$$O_{\tilde{I}} = O + O\tilde{I}, \tag{3}$$

The maximum ligand-reflection group (A + D):

$$O_{\hat{I}} = O+O\hat{I}, \tag{4}$$

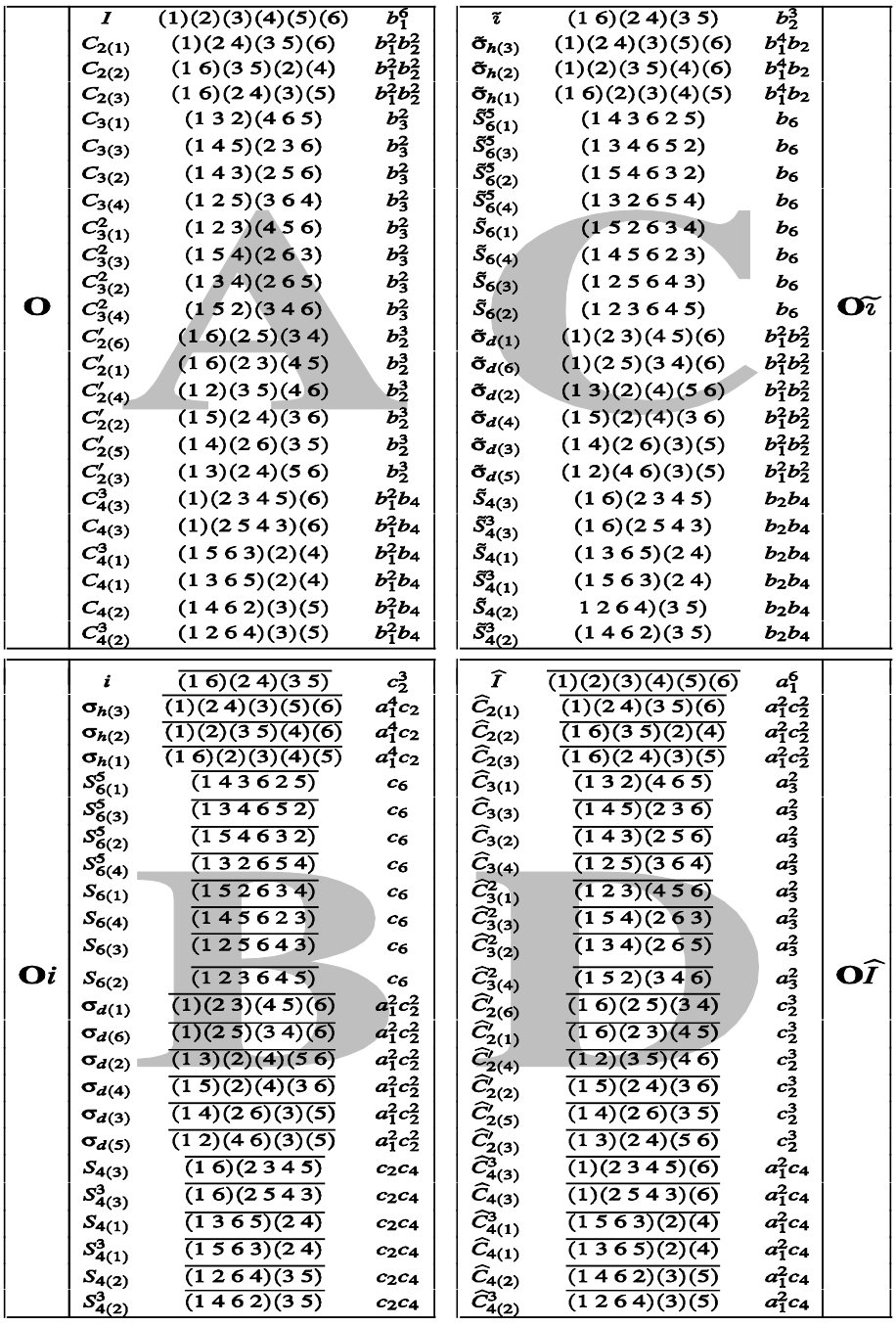

Figure 2. *RS*-Stereoisomeric group $O_{h\tilde{I}\hat{I}}$ for an octahedral skeleton. The elements of the coset O (= O*I*) are called *rotations*, the elements of the coset O*i* are called (*roto*) *reflections*, the elements of the coset $O\tilde{I}$ are called *RS-permutations*, and the elements of the coset $O\hat{I}$ are called *ligand reflections*.[33]

where these subgroups of order 48 contain the point group O of order 24 commonly. It should be noted that the *RS*-stereoisomeric group $O_{h\tilde{I}\hat{I}}$ contains other subgroups of order 48, which do not contain the point group O of order 24. For example, the *RS*-stereoisomeric group $T_{d\tilde{\sigma}\hat{I}}$ derived from the point group T_d (cf. Table 1 of [21]) is of order 48 and does not contain O, although it is a subgroup of $O_{h\tilde{I}\hat{I}}$.

According to Eqs. 1, 2, 3, and 4 in addition to the common chiral subgroup O, a subgroup G of the *RS*-stereoisomeric group $O_{h\tilde{I}\hat{I}}$ is classified into one of the following five types:

$$\begin{aligned}
&\text{type I:} && G \subset O_{\hat{I}} \quad (G \not\subset O)\\
&\text{type II:} && G \subset O_{\tilde{I}} \quad (G \not\subset O)\\
&\text{type III:} && G \subset O\\
&\text{type IV:} && G \subset O_{h\tilde{I}\hat{I}} \quad (G \not\subset O, G \not\subset O_{\tilde{I}}, G \not\subset O_{\hat{I}}, G \not\subset O_h)\\
&\text{type V:} && G \subset O_h \quad (G \not\subset O)
\end{aligned} \tag{5}$$

2.2. STEREOISOGRAMS AS DIAGRAMMATIC EXPRESSIONS OF RS-STEREOISOMERIC GROUPS

The four skeletons collected in Figure 1 are interchanged into one another on the action of the *RS*-stereoisomeric group $O_{h\tilde{I}\hat{I}}$ (Eq. 1) and its subgroups listed in Eqs. 2, 3, and 4. In general, a quadruplet of four skeletons linked with double-headed arrows (e.g., Figure 1) is called *an elementary stereoisogram*. The elementary stereoisogram of octahedral skeletons (Figure 1) is a basic diagram for giving stereoisograms of octahedral derivatives as promolecules, where a set of proligands (abstract ligands with chirality/achirality, e.g, A, B, C, X, Y, and Z for achiral proligands, as well as $p/\overline{p}$, $q/\overline{q}$, $r/\overline{r}$, and $s/\overline{s}$ for a pair of chiral proligands of opposite chirality senses) is placed on the six positions of each of the skeletons, as exemplified in Figure 3. Note that an achiral proligand (e.g., A) on a position with an overlined number (e.g., 1) remains unchanged, because $\overline{A}$ is identical with A itself. On the other hand, a chiral proligand (e.g., p or $\overline{p}$) on a position with an overlined number (e.g., $\overline{1}$) is changed into its mirror-image proligand (e.g., $\overline{p}$ or p), where $\overline{\overline{p}} = p$

Each of the resulting quadruplets of promolecules (octahedral derivatives) belongs to a subgroup G of the *RS*-stereoisomeric group $O_{h\tilde{I}\hat{I}}$, so that it is characterized to be one of five types (type I to type V). In other words, each stereoisogram can be categorized into one of type I to type V, as shown in Figure 3.

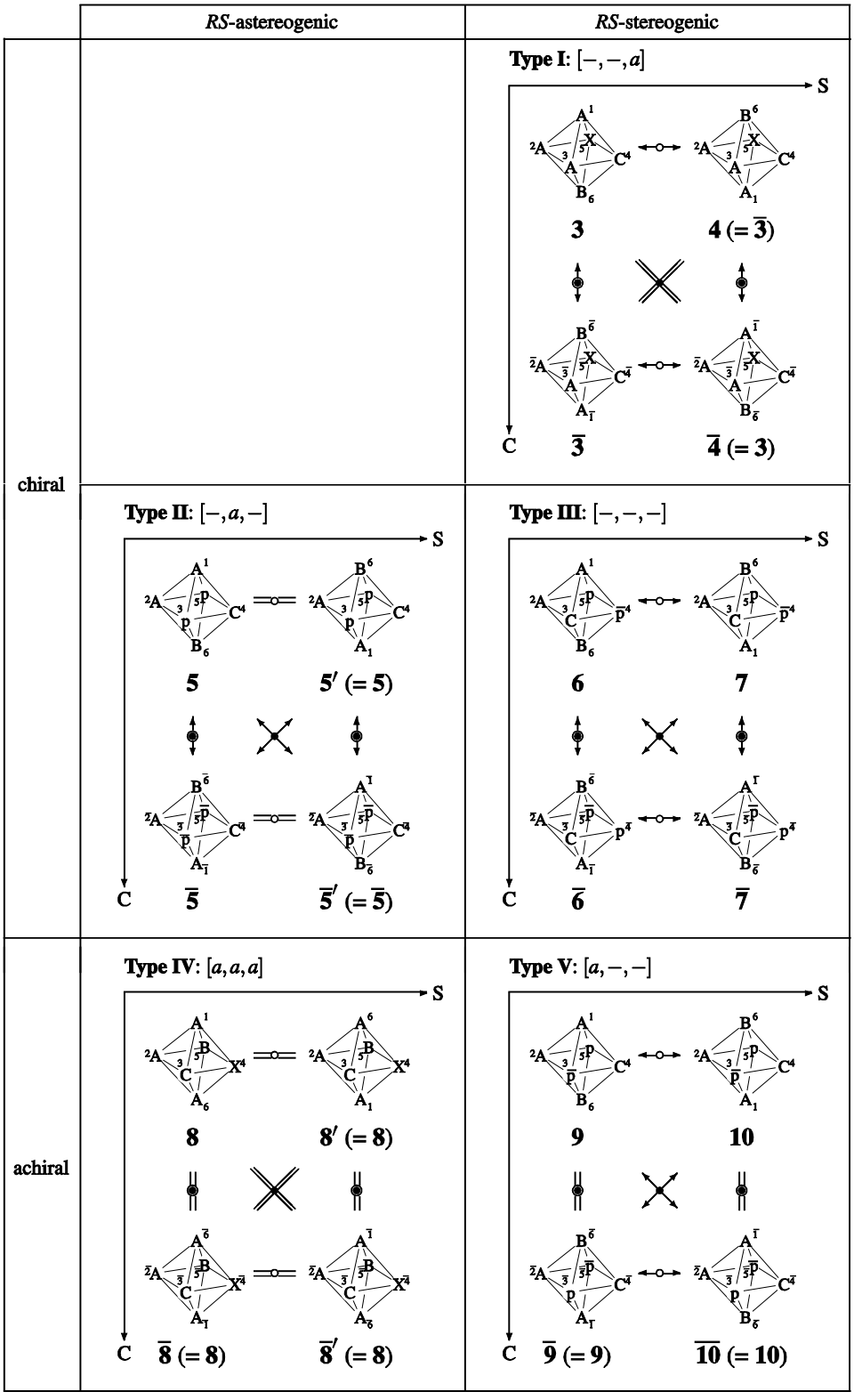

Figure 3. Stereoisograms for representing *RS*-stereoisomers of five types [4].

For the purpose of applying *RS*-stereoisomeric groups to qualitative discussions, the following terminology based on stereoisograms is adopted [34].

1. The relationship between 1 and $\bar{1}$ (or between 2 and $\bar{2}$) in the vertical direction of Figure 1 is called a (self-)enantiomeric relationship, where the corresponding attribute is called chirality (or achirality). The interconversion between 1 and $\bar{1}$ (or between 2 and $\bar{2}$) is brought about by reflections contained in the point group O_h,
2. The relationship between 1 and 2 (or between $\bar{1}$ and $\bar{2}$) in the horizontal direction of Figure 1 is called a (self-)*RS*-diastereomeric relationship, where the corresponding attribute is called *RS*-stereogenicity (or *RS*-astereogenicity). The interconversion between 1 and 2 (or between $\bar{1}$ and $\bar{2}$) is brought about by *RS*-permutations contained in the *RS*-permutation group $O_{\tilde{I}}$.
3. The relationship between 1 and $\bar{2}$ (or between 2 and $\bar{1}$) in the diagonal direction of Figure 1 is called a (self-)holantimeric relationship, where the corresponding attribute is called sclerality (or asclerality). The interconversion between 1 and $\bar{2}$ (or between 2 and $\bar{1}$) is brought about by ligand reflections contained in the ligand-reflection group $O_{\hat{I}}$.

A type-I stereoisogram is characterized by equality symbols in the diagonal direction, so that the enantiomeric relationship is coincident with the *RS*-diastereomeric relationship in the type-I stereoisogram (cf. Figure 3). This means that the quadruplet of promolecules contained in the type-I stereoisogram belongs to a type-I subgroup shown in Eq. 5. For example, the promolecule 3 is identical with its holantimer $\bar{4}$ (= 3), so that it is self-holantimeric and exhibits asclerality. According to the terminology described above, the type-I stereoisogram is chiral, *RS*-stereogenic, and ascleral, so that it is characterized by a type index [−,−,*a*].

A type-II stereoisogram is characterized by equality symbols in the horizontal direction, so that the enantiomeric relationship is coincident with the holantimeric relationship in the type- II stereoisogram (cf. Figure 3). This means that the quadruplet of promolecules contained in the type-II stereoisogram belongs to a type-II subgroup shown in Eq. 5. For example, the promolecule 5 is identical with its *RS*-diastereomer $5'$ (= 5) so that it is self-*RS*-diastereomeric and exhibits *RS*-astereogenicity. According to the terminology described above, the type-II stereoisogram is chiral, *RS*-astereogenic, and scleral, so that it is characterized by a type index [−,*a*,−].

A type-III stereoisogram is characterized by the absence of equality symbols in all directions, so that it belongs to a type-III subgroup shown in Eq. 5. For example, the

promolecules 6, 7, $\overline{6}$, and $\overline{7}$ are different from one another (Figure 3). Hence, the type-III stereoisogram is chiral, *RS*-stereogenic, and scleral, so that it is characterized by a type index [−,−,−].

A type-IV stereoisogram is characterized by the presence of equality symbols in all directions, so that it belongs to a type-IV subgroup shown in Eq. 5. For example, the promolecules 8, $8'$, $\overline{8}$ and $\overline{8}'$ are identical with one another (Figure 3). Hence, the type-IV stereoisogram is achiral, *RS*-astereogenic, and ascleral, so that it is characterized by a type index [*a*,*a*,*a*].

A type-V stereoisogram is characterized by equality symbols in the vertical direction, so that the *RS*-diastereomeric relationship is coincident with the holantimeric relationship in the type-V stereoisogram (cf. Figure 3). This means that the quadruplet of promolecules contained in the type-V stereoisogram belongs to a type-V subgroup shown in Eq. 5. For example, the promolecule 9 (or 10) is identical with its enantiomer $\overline{9}$ (= 9) (or $\overline{10}$ (= 10)), so that it is self-enantiomeric and exhibits achirality. The relationship between 9 and 10 is an *RS*-diastereomeric relationship. According to the terminology described above, the type-V stereoisogram is achiral, *RS*-stereogenic, and scleral, so that it is characterized by a type index [*a*,–,–]. Such a pair of *RS*-diastereomers is referred to under the term 'pseudoasymmetry' in the conventional terminology of stereochemistry.

3. GROSS ENUMERATION

3.1. ACTION OF THE MAXIMUM POINT GROUP O_h

The symmetry-itemized enumeration of octahedral complexes has been conducted by Fujita's USCI approach [35]. Because the inverse mark table and the USCI-CF table of O_h has been reported in [36, 28], Def. 16.1 of [19] for gross enumeration can be applied to the gross enumeration of octahedral complexes. According to Section 2.6 of [28], the procedure of gross enumeration can be simplified by using a gross enumeration matrix (GEM), where the column sum $\hat{N}$ of the inverse mark table is beforehand evaluated (Theorem 2.8 of [28]). Thus, the column sum $\hat{N}$ for O_h is calculated as follows:

$$T_{\hat{N}} = (\frac{1}{48},\frac{1}{16},\frac{1}{8},\frac{1}{16},\frac{1}{8},\frac{1}{48},\frac{1}{6},\frac{1}{8},\frac{1}{8},0,0,0,0,0,0, \\ 0,0,0,\frac{1}{6},0,0,0,0,0,0,0,0,0,0,0,0,0,0), \tag{6}$$

which is cited from Table 3 of [36] or Table 2.4 of [28].

The six positions of the octahedral skeleton construct an orbit governed by the coset representation $O_h(/C_{4v})$, which is listed as products of cycles in the left parts (A and B) of

Figure 2. Hence, the $O_h(/C_{4v})$-row of the USCI-CF table of O_h (Tables 4 and 5 of [36] or Tables 2.5 and 2.6 of [28]) is adopted and aligned to form a formal row vector as follows:

$$\begin{aligned}\mathrm{USCI\text{-}CF}_{O_h(/C_{4v})} = (&b_1^6, b_1^2b_2^2, b_2^3, a_1^4c_2, a_1^2c_2^2, c_2^3, b_3^2, b_1^2b_4, c_2c_4, b_2^3,\\ &b_2b_4, a_1^2a_2^2, a_1^2c_4, a_2^3, a_2^2c_2, a_2c_4, b_6, a_3^2, c_6, b_2b_4,\\ &a_1^2a_4, c_2a_4, a_2c_4, a_2a_4, a_2^3, a_2a_4, b_6, a_6, a_2a_4, b_6, a_6, a_6, a_6).\end{aligned} \tag{7}$$

According to Corollary 1.3 of [37], the formal row vector $\mathrm{USCI\text{-}CF}_{O_h(/C_{4v})}$ (Eq. 7) is multiplied by the column vector (Eq. 6), so as to give the corresponding CI-CF as follows:

$$\begin{aligned}\mathrm{CI\text{-}CF}_{O_h(/C_{4v})} &= \mathrm{USCI\text{-}CF}_{O_h(/C_{4v})} \times \hat{N}\\ &= \frac{1}{48}b_1^6 + \frac{1}{16}b_1^2b_2^2 + \frac{1}{8}b_2^3 + \frac{1}{16}a_1^4c_2 + \frac{1}{8}a_1^2c_2^2\\ &+ \frac{1}{48}c_2^3 + \frac{1}{6}b_3^2 + \frac{1}{8}b_1^2b_4 + \frac{1}{8}c_2c_4 + \frac{1}{6}c_6.\end{aligned} \tag{8}$$

The CI-CF can be alternatively obtained according to Fujita's proligand method [38, 39,40], which has been introduced in a book (Chapter 7 of [28]). Let us start from the coset representation $O_h(/C_{4v})$ listed as products of cycles in the left parts (A and B) of Figure 2. Each cycle is classified into one of three categories, i.e., homospheric, enantiospheric, and hemispheric cycles, where the concept of sphericities for cycles is introduced in a similar way to the concept of sphericities for orbits. Then, a product of sphericity indices (PSI) is calculated for characterizing each product of cycles, where a sphericity index a_d is assigned to a homospheric d-cycle, a sphericity index c_d is assigned to an enantiospheric d-cycle, and a sphericity index b_d is assigned to a hemispheric d-cycle.

For example, the two-fold rotation $C_{2(1)}$ represented by a product of cycles (1)(2 4)(3 5)(6) (Figure 2) is characterized by a PSI $b_1^2b_2^2$, because each of the two 1-cycles is hemispheric and takes SI b_1, while each of the two 2-cycles is hemispheric and takes SI b_2. The reflection $\sigma_{h(3)}$ represented by a product of cycles $\overline{(1)(2\ 4)(3)(5)(6)}$ is characterized by a PSI $a_1^4c_2$, because each of the four 1-cycles is homospheric and takes SI a_1, while the one 2-cycles is enantiospheric and takes SI c_2. The resulting PSIs are listed in the rightmost column of each part of Figure 2.

According to Fujita's proligand method [38, 39, 40], all of the PSIs for the point group O_h (the parts A and B of Figure 2) are summed up. The resulting sum is divided by the order of O_h (48), so as to give the following CI-CF (Def. 7.20 of [28]):

$$\mathrm{CI\text{-}CF}(\mathrm{O}_h) = \frac{1}{48}(b_1^6 + 3b_1^2b_2^2 + 8b_3^2 + 6b_2^3 + 6b_1^2b_4 + c_2^3 + 3a_1^4c_2 + 8c_6 + 6a_1^2c_2^2 + 6c_2c_4), \tag{9}$$

which is identical with Eq. 8. A general treatment of CI-CFs for maximum point groups has been reported (Eq. 27 of [30]).

To enumerate octahedral derivatives (promolecules), six proligands are selected from an inventory of proligands:

$$\mathrm{X} = \{\mathrm{A}, \mathrm{B}, \mathrm{C}, \mathrm{X}, \mathrm{Y}, \mathrm{Z}; \mathrm{p}, \bar{\mathrm{p}}, \mathrm{q}, \bar{\mathrm{q}}, \mathrm{r}, \bar{\mathrm{r}}, \mathrm{s}, \bar{\mathrm{s}}, \mathrm{u}, \bar{\mathrm{u}}, \mathrm{v}, \bar{\mathrm{v}}\}, \tag{10}$$

where the letters A, B, C, X, Y, and Z represent achiral proligands and the pairs of $\mathrm{p}/\bar{\mathrm{p}}$, $\mathrm{q}/\bar{\mathrm{q}}$, $\mathrm{r}/\bar{\mathrm{r}}$, $\mathrm{s}/\bar{\mathrm{s}}$, $\mathrm{u}/\bar{\mathrm{u}}$, and $\mathrm{v}/\bar{\mathrm{v}}$ represent pairs of enantiomeric proligands in isolation (when detached). A set of six proligands selected from the ligand inventory X is placed on the six positions of an octahedral skeleton 1.

According to Theorem 1 of [38] (Theorem 7.21 of [28]), we use the following ligand-inventory functions:

$$a_d = \mathrm{A}_d + \mathrm{B}_d + \mathrm{C}_d + \mathrm{X}_d + \mathrm{Y}_d + \mathrm{Z}_d \tag{11}$$

$$c_d = \mathrm{A}^d + \mathrm{B}^d + C^d + X^d + Y^d + Z^d + 2p^{d/2}\,\bar{p}^{d/2} + 2q^{d/2}\bar{q}^{d/2} + 2r^{d/2}\bar{r}^{d/2} + 2s^{d/2}\bar{s}^{d/2} + 2u^{d/2}\bar{u}^{d/2} + 2v^{d/2}\bar{v}^{d/2} \tag{12}$$

$$b_d = \mathrm{A}^d + \mathrm{B}^d + X^d + Y^d + p^d + q^d + r^d + s^d + u^d + v^d + \bar{p}^d + \bar{q}^d + \bar{r}^d + \bar{s}^d + \bar{u}^d + \bar{v}^d. \tag{13}$$

These ligand-inventory functions are introduced into an CI-CF represented by Eq. 9 (or Eq. 8). The resulting equation is expanded to give a generating function, in which the coefficient of the term $\mathrm{A}^a\,\mathrm{B}^b\,\mathrm{C}^c\,\mathrm{X}^x\,\mathrm{Y}^y\,\mathrm{Z}^z\,\mathrm{p}^p\,\bar{\mathrm{p}}^{\bar{p}}\,\mathrm{q}^q\,\bar{\mathrm{q}}^{\bar{q}}\,\mathrm{r}^r\,\bar{\mathrm{r}}^{\bar{r}}\,\mathrm{s}^s\,\bar{\mathrm{s}}^{\bar{s}}\,\mathrm{u}^u\,\bar{\mathrm{u}}^{\bar{u}}\,\mathrm{v}^v\,\bar{\mathrm{v}}^{\bar{v}}$ indicates the number of pairs of enantiomeric promolecules (or achiral promolecules) to be counted. Note that the enumeration under the point group O_h (using Eq. 9) counts each enantiomeric pair (or each achiral promolecule) just once.

Because the proligands A, B, etc. appear symmetrically, the term can be represented by the following partition:

$$[\theta] = [a, b, c, x, y, z; p, \bar{p}, q, \bar{q}, r, \bar{r}, s, \bar{s}, u, \bar{u}, v, \bar{v}], \tag{14}$$

where we put $a \geq b \geq c \geq x \geq y \geq z$; $p \geq \bar{p}$, $q \geq \bar{q}$, $r \geq \bar{r}$, $s \geq \bar{s}$, $u \geq \bar{u}$, $v \geq \bar{v}$; and $p \geq q \geq r \geq s \geq u \geq v$ without losing generality. For example, the partitions:

$$[\theta]_1 = [6,0,0,0,0,0,0,0,0,0,0,0,0,0,0,0,0,0] \tag{15}$$

$$[\theta]_2 = [5,1,0,0,0,0,0,0,0,0,0,0,0,0,0,0,0,0] \text{ , etc} \tag{16}$$

correspond to the terms A^6, B^6 ...; A^5B, A^5C, ...; and so on.

3.2. ACTION OF THE MAXIMUM CHIRAL SUBGROUP O

Enumeration under the action of the maximum chiral subgroup is referred to as enumeration of promolecules as steric isomers in Chapter 7 of [28]. The enumeration of octahedral promolecules as steric isomers is conducted under the point group O, so that the CI-CF for is calculated by using the PSIs collected in the upperleft part of Figure 2 according to Def. 7.23 of [28] as follows:

$$\mathrm{CI\text{-}CF(O)} = \frac{1}{24}(b_1^6 + 3b_1^2b_2^2 + 8b_3^2 + 6b_2^3 + 6b_1^2b_4). \tag{17}$$

A general treatment of CI-CFs for maximum chiral subgroups has been reported (Eq. 17 of [29]).

The ligand-inventory function represented by Eq. 13 is introduced into Eq. 17. The resulting equation is expanded to give a generating function. Note that the enumeration under the maximum chiral point group O (using Eq. 17) counts each promolecule of an enantiomeric pair (or each achiral promolecule) just once.

3.3 ACTION OF THE MAXIMUM RS-PERMUTATION GROUP $O_{\tilde{I}}$

The point group T_d and the symmetric group of degree 4 $S^{[4]}$ are compared by applying them to a tetrahedral skeleton [41], although the concept of *RS*-stereoisomeric groups was not developed at that time. Note that the symmetric group of degree 4 $S^{[4]}$ is regarded as an *RS*-permutation group $T_{\tilde{\sigma}}$ from the viewpoint of Fujita's stereoisogram approach [3, 1].

Enumeration under the *RS*-permutation group $O_{\tilde{I}}$ can be conducted in a parallel way. Thus, all of the PSIs for the *RS*-permutation group $O_{\tilde{I}}$ (the parts A and C of Figure 2) are summed up. The resulting sum is divided by the order of $O_{\tilde{I}}$ (48), so as to give the following CI-CF:

$$\begin{aligned}\mathrm{CI\text{-}CF}(O_{\tilde{I}}) = \frac{1}{48}(&b_1^6 + 3b_1^2b_2^2 + 8b_3^2 + 6b_2^3 + 6b_1^2b_4 \\ &+ b_2^3 + 3b_1^4b_2 + 8b_6 + 6b_1^2b_2^2 + 6b_2b_4).\end{aligned} \tag{18}$$

A general treatment of CI-CFs for maximum *RS*-permutation groups has been reported (Eq. 41 of [30]).

The ligand-inventory function represented by Eq. 13 is introduced into Eq. 18. The resulting equation is expanded to give a generating function. Note that the enumeration under the *RS*-permutation group $O_{\tilde{I}}$ (using Eq. 18) counts a pair of *RS*-diastereomers (or each *RS*-astereogenic promolecule) just once.

3.4. ACTION OF THE MAXIMUM LIGAND-REFLECTION GROUP $O_{\hat{I}}$

To conduct enumeration under the maximum ligand-reflection group $O_{\hat{I}}$, all of the PSIs for $O_{\hat{I}}$ (the parts A and D of Figure 2) are summed up. The resulting sum is divided by the order of $O_{\hat{I}}$ (48), so as to give the following CI-CF:

$$\begin{aligned} \mathrm{CI\text{-}CF}(O_{\hat{I}}) = \frac{1}{48}(&b_1^6 + 3b_1^2b_2^2 + 8b_3^2 + 6b_2^3 + 6b_1^2b_4 \\ &+ a_1^6 + 3a_1^2c_2^2 + 8a_3^2 + 6c_2^3 + 6a_1^2c_4). \end{aligned} \tag{19}$$

A general treatment of CI-CFs for maximum ligand-reflection groups has been reported (Eq. 54 of [30]).

The ligand inventory functions represented by Eqs. 11–13 are introduced into Eq. 19. The resulting equation is expanded to give a generating function. Note that the enumeration under the maximum ligand-reflection group $O_{\hat{I}}$, (using Eq. 19) counts a pair of holantimers (or each *RS*-ascleral promolecule) just once.

3.5. ACTION OF THE RS-STEREOISOMERIC GROUP $O_{h\tilde{I}\hat{I}}$

Because products of cycles appearing in the lower parts (B and D) of Figure 2 contain ligand reflections as designated by overbars, they are characterized by products of a_d and/or c_d after the concept of sphericities for cycles is extended to meet *RS*-stereoisomeric groups [30]. Thereby, Fujita's proligand method [38, 39, 40] is extended to evaluate the number of quadruplets of *RS*-stereoisomeric promolecules. The following cycle index with chirality fittingness (CI-CF) is obtained:

$$\begin{aligned} \mathrm{CI\text{-}CF}(O_{h\tilde{I}\hat{I}}) = \frac{1}{96}(&b_1^6 + 3b_1^2b_2^2 + 8b_3^2 + 6b_2^3 + 6b_1^2b_4 \\ &+ c_2^3 + 3a_1^4c_2 + 8c_6 + 6a_1^2c_2^2 + 6c_2c_4 \\ &+ b_2^3 + 3b_1^4b_2 + 8b_6 + 6b_1^2b_2^2 + 6b_2b_4 \\ &+ a_1^6 + 3a_1^2c_2^2 + 8a_3^2 + 6c_2^3 + 6a_1^2c_4). \end{aligned} \tag{20}$$

A general treatment of CI-CFs for *RS*-stereoisomeric groups has been reported (Eq. 11 of [30]).

The ligand inventory functions represented by Eqs. 11–13 are introduced into Eq. 20. The resulting equation is expanded to give a generating function. Note that the enumeration under the *RS*-stereoisomeric group $O_{h\tilde{I}\hat{I}}$ (using Eq. 20) counts a quadruplet of *RS*-stereoisomers (type I to type V) just once.

4. TYPE-ITEMIZED ENUMERATION

4.1. FOUNDATIONS FOR CI-CFS OF FIVE TYPES

Under the *RS*-stereoisomeric group $O_{h\tilde{I}\hat{I}}$, a quadruplet of *RS*-stereoisomers contained in a stereoisogram (type I to type V) is an equivalence class, which is counted just once by means of the CI-CF represented by Eq. 20. Let the symbol CI-CF$^{[K]}$($O_{h\tilde{I}\hat{I}}$) (K = I, II, . . . V) be a CI-CF for counting each type. Then, their sum is equal to Eq. 20 as follows:

$$\begin{aligned} \text{CI-CF}(\text{O}_{h\tilde{I}\hat{I}}) = {} & \text{CI-CF}^{[\text{I}]}(\text{O}_{h\tilde{I}\hat{I}}) + \text{CI-CF}^{[\text{II}]}(\text{O}_{h\tilde{I}\hat{I}}) + \text{CI-CF}^{[\text{III}]}(\text{O}_{h\tilde{I}\hat{I}}) \\ & + \text{CI-CF}^{[\text{IV}]}(\text{O}_{h\tilde{I}\hat{I}}) + \text{CI-CF}^{[\text{V}]}(\text{O}_{h\tilde{I}\hat{I}}) \end{aligned} \tag{21}$$

Under the maximum chiral subgroup O, each promolecule of an enantiomeric pair (or each achiral promolecule) is an equivalence class, which is counted just once by means of the CI-CF represented by Eq. 17. Figure 3 indicates that a type-I stereoisogram contains two promolecules, a type-II stereoisogram contains two promolecules, a type-III stereoisogram contains four promolecules, a type-IV stereoisogram contains one promolecule, and a type-V stereoisogram contains two promolecules. Hence, the CI-CF of Eq. 17 is represented as follows:

$$\begin{aligned} \text{CI-CF}(\text{O}) = {} & 2\text{CI-CF}^{[\text{I}]}(\text{O}_{h\tilde{I}\hat{I}}) + 2\text{CI-CF}^{[\text{II}]}(\text{O}_{h\tilde{I}\hat{I}}) + 4\,\text{CI-CF}^{[\text{III}]}(\text{O}_{h\tilde{I}\hat{I}}) \\ & + \text{CI-CF}^{[\text{IV}]}(\text{O}_{h\tilde{I}\hat{I}}) + 2\,\text{CI-CF}^{[\text{V}]}(\text{O}_{h\tilde{I}\hat{I}}). \end{aligned} \tag{22}$$

Under the maximum point group O_h, each pair of (self-)enantiomers is an equivalence class, which is counted just once by means of the CI-CF represented by Eq. 9. Note that a pair of self-enantiomers means an achiral promolecule. Figure 3 indicates that a type-I stereoisogram contains one pair of enantiomers, a type-II stereoisogram contains one pair of enantiomers, a type-III stereoisogram contains two pairs of enantiomers, a type-IV stereoisogram contains one pair of self-enantiomers (one achiral promolecule), and a type-V stereoisogram contains two pairs of self-enantiomers (two achiral promolecules). Hence, the CI-CF of Eq. 9 is represented as follows:

$$\begin{aligned} \text{CI-CF}(\text{O}_h) = {} & \text{CI-CF}^{[\text{I}]}(O_{h\tilde{I}\hat{I}}) + \text{CI}-\text{CF}^{[\text{II}]}(\text{O}_{h\tilde{I}\hat{I}}) + 2\,\text{CI}-\text{CF}^{[\text{III}]}(\text{O}_{h\tilde{I}\hat{I}}) \\ & + \text{CI}-\text{CF}^{[\text{IV}]}(\text{O}_{h\tilde{I}\hat{I}}) + 2\text{CI}-\text{CF}^{[\text{V}]}(\text{O}_{h\tilde{I}\hat{I}}) \end{aligned} \tag{23}$$

Under the maximum *RS*-permutation group $\text{O}_{\tilde{I}}$, each pair of (self-)*RS*-diastereomers is an equivalence class, which is counted just once by means of the CI-CF represented by Eq. 18. Note that a pair of self-*RS*-diastereomers means an *RS*-astereogenic promolecule. Figure 3 indicates that a type-I stereoisogram contains one pair of *RS*-diastereomers, a type-II stereoisogram contains two pairs of self-*RS*-diastereomers (two *RS*-astereogenic

promolecules), a type- III stereoisogram contains two pairs of *RS*-diastereomers, a type-IV stereoisogram contains one pair of self-*RS*-diastereomers (one *RS*-astereogenic promolecule), and a type-V stereoisogram contains one pair of *RS*-diastereomers. Hence, the CI-CF of Eq. 18 is represented as follows:

$$\begin{aligned} \text{CI-CF}(O_{\tilde{I}}) = {} & \text{CI-CF}^{[\text{I}]}(O_{h\tilde{I}\hat{I}}) + 2\text{CI-CF}^{[\text{II}]}(O_{h\tilde{I}\hat{I}}) + 2\text{CI-CF}^{[\text{III}]}(O_{h\tilde{I}\hat{I}}) \\ & + \text{CI-CF}^{[\text{IV}]}(O_{h\tilde{I}\hat{I}}) + \text{CI-CF}^{[\text{V}]}(O_{h\tilde{I}\hat{I}}). \end{aligned} \tag{24}$$

Under the maximum ligand-reflection group $O_{\hat{I}}$, each pair of (self-)holantimers is an equivalence class, which is counted just once by means of the CI-CF represented by Eq. 19. Note that a pair of self-holantimers means an ascleral promolecule. Figure 3 indicates that a type-I stereoisogram contains two pairs of self-holantimers (two ascleral promolecules), a type-II stereoisogram contains one pair of holantimers, a type-III stereoisogram contains two pairs of holantimers, a type-IV stereoisogram contains one pair of self-holantimers (one ascleral promolecule), and a type-V stereoisogram contains one pair of holantimers. Hence, the CI-CF of Eq. 19 is represented as follows:

$$\begin{aligned} \text{CI-CF}(O_{\hat{I}}) = {} & 2\,\text{CI-CF}^{[\text{I}]}(O_{h\tilde{I}\hat{I}}) + \text{CI-CF}^{[\text{II}]}(O_{h\tilde{I}\hat{I}}) + 2\text{CI-CF}^{[\text{III}]}(O_{h\tilde{I}\hat{I}}) \\ & + \text{CI-CF}^{[\text{IV}]}(O_{h\tilde{I}\hat{I}}) + \text{CI-CF}^{[\text{V}]}(O_{h\tilde{I}\hat{I}}). \end{aligned} \tag{25}$$

Although the five equations (Eqs. 21, 22, 23, 24, and 25) are obtained, they cannot be solved to give $\text{CI-CF}^{[\text{K}]}(O_{h\tilde{I}\hat{I}})$ (K = I, II, . . . V).

For the purpose of obtaining $\text{CI-CF}^{[\text{k}]}(O_{h\tilde{I}\hat{I}})$ For the purpose of obtaining $\text{CI-CF}^{[\text{k}]}(O_{h\tilde{I}\hat{I}})$ (K = I, II, . . . V), the CI-CF of Eq. 23 is modulated according to Def. 1 of [32].) (K = I, II, . . . V), the CI-CF of Eq. 23 is modulated according to Def. 1 of [32].

$$\begin{aligned} \text{CI-CF}''(O_h) = {} & \text{CI-CF}(O_h) - \text{CI-CF}^{[\text{V}]}(O_{h\tilde{I}\hat{I}}) \\ = {} & \text{CI-CF}^{[\text{I}]}(O_{h\tilde{I}\hat{I}}) + \text{CI-CF}^{[\text{II}]}(O_{h\tilde{I}\hat{I}}) + 2\text{CI-CF}^{[\text{III}]}(O_{h\tilde{I}\hat{I}}) \\ & + \text{CI-CF}^{[\text{IV}]}(O_{h\tilde{I}\hat{I}}) + \text{CI-CF}^{[\text{V}]}(O_{h\tilde{I}\hat{I}}). \end{aligned} \tag{26}$$

If the modulated $\text{CI-CF}''(O_h)$ is evaluated, Eqs. 21, 22, 24, and 25 in addition to Eq. 26 can be solved to give $\text{CI-CF}^{[\text{K}]}(O_{h\tilde{I}\hat{I}})$ (K = I, II, . . . V) as follows:

$$\text{CI-CF}^{[\text{I}]}(O_{h\tilde{I}\hat{I}}) = -\text{CI-CF}''(O_h) + \text{CI-CF}(O_{\hat{I}}) \tag{27}$$

$$\text{CI-CF}^{[\text{II}]}(O_{h\tilde{I}\hat{I}}) = -\text{CI-CF}''(O_h) + \text{CI-CF}(O_{\tilde{I}}) \tag{28}$$

$$\text{CI-CF}^{[\text{III}]}(O_{h\tilde{I}\hat{I}}) = \text{CI-CF}''(O_h) - \text{CI-CF}(O_{h\tilde{I}\hat{I}}) \tag{29}$$

$$\text{CI-CF}^{[\text{IV}]}(O_{h\tilde{I}\hat{I}}) = -\text{CI-CF}(O) + 2\text{CI-CF}''(O_h) \tag{30}$$

$$\text{CI-CF}^{[V]}(O_{h\tilde{I}\hat{I}}) = \text{CI-CF}(O) - \text{CI-CF}''(O_h) - \text{CI-CF}(O_{\tilde{I}}) - \text{CI-CF}(O_{\hat{I}}) + 2\text{CI-CF}(O_{h\tilde{I}\hat{I}}) \quad (31)$$

Note that the introduction of CI-CF″(O_h) (Eq. 26) into Eq. 31 generates the following equation:

$$\text{CI-CF}(O) = \text{CI-CF}(O_h) + \text{CI-CF}(O_{\tilde{I}}) + \text{CI-CF}(O_{\hat{I}}) - 2\text{CI-CF}(O_{h\tilde{I}\hat{I}}), \quad (32)$$

which is an identical equation.

4.2. EVALUATION OF THE MODULATED CI-CF

The next task is the evaluation of the modulated CI-CF shown in Eq. 26. By starting from Eqs. 22 and 23 and by introducing Eqs. 9 and 17, we obtain the following CI-CF:

$$\text{CI-CF}^{[IV]}(O_{h\tilde{I}\hat{I}}) + 2\text{CI-CF}^{[V]}(O_{h\tilde{I}\hat{I}}) = 2\text{CI-CF}(O_h) - \text{CI-CF}(O) = \frac{1}{24}(c_2^3 + 3a_1^4c_2 + 8c_6 + 6a_1^2c_2^2 + 6c_2c_4), \quad (33)$$

which indicates that achiral promolecules (type IV plus 2× type V) are counted under the point group O_h. For the purpose of evaluating $\text{CI-CF}^{[V]}(O_{h\tilde{I}\hat{I}})$, let us examine whether or not each term appearing in the right-hand side of Eq. 33 contributes the formation of type-V promolecules.

The term c_2^3 (a PSI) in Eq. 33 is concerned with the generation of such a type-V promolecule as having the composition $p\bar{p}q\bar{q}r\bar{r}$, which is depicted in Figure 4. The generating function which is generated by introducing the ligand-inventory function of Eq. 12 into the PSI c_2^3 is contaminated with terms of type-IV promolecules, which stem from the PSIs such as $a_2c_2^2, a_2^2c_2, c_2c_4, a_2c_4, a_4c_2, a_2a_4, c_6, a_6$ and c_2^3, because each c_2 in the PSI c_2^3 behaves independently.

The influences of such contaminated PSIs are excluded by trial-and-error examination of inclusion-exclusion behaviors, so as to leave such necessary terms as $p\bar{p}q\bar{q}r\bar{r}$. The source code based on the GAP system is attached as an appendix, where a simplified examination is executed by using the ligand-inventory functions with A, B, C, X, $p/\bar{p}$, $q/\bar{q}$, and $r/\bar{r}$. Thereby, the following equation is obtained as a net contribution of c_2^3 to type V:

$$V_1 := \frac{1}{48}(c_2^3 - 3(a_2c_2^2 - a_2^2c_2) - 6(c_2c_4 - a_2c_4 - a_4c_2 + a_2a_4) + 8(c_6 - a_6) - a_2^3), \quad (34)$$

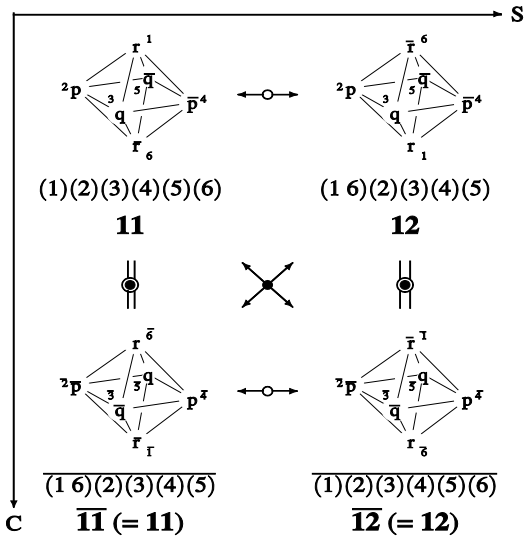

Figure 4. Type-V stereoisogram of a promolecule with the composition $p\bar{p}q\bar{q}r\bar{r}$, which is evaluated by the PSI c_2^3.

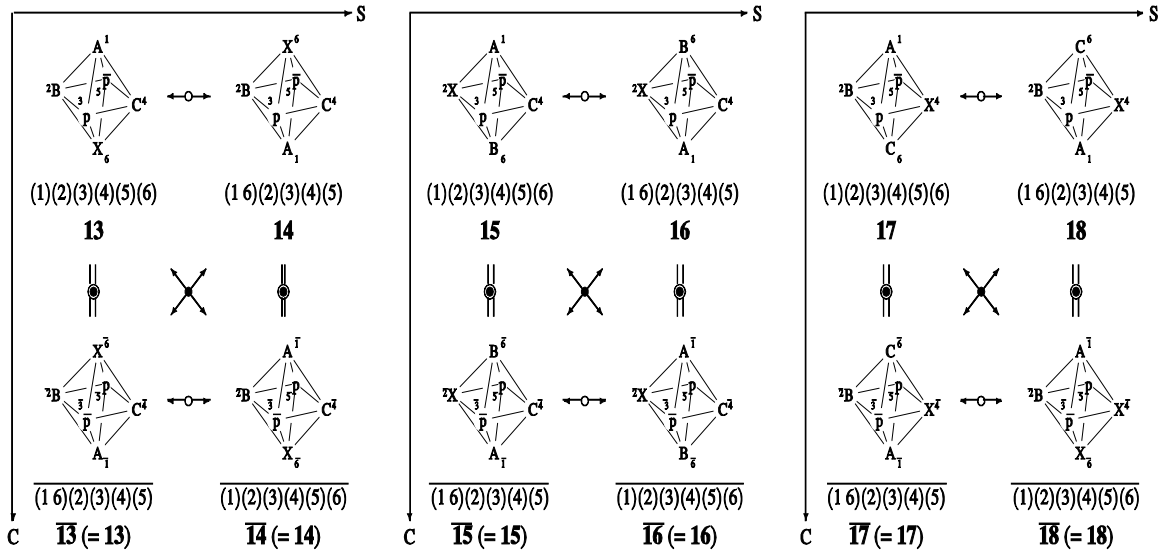

.

Figure 5. Type-V stereoisograms of promolecules with the composition $ABCXp\,\bar{p}$, which are evaluated by the PSI $a_1^4 c_2$.

which leaves such necessary terms as $p\bar{p}q\bar{q}r\bar{r}$. The term $3a_1^4 c_2$ in Eq. 33 is concerned with the generation of such type-V promolecules as having the composition $A^2BCp\,\bar{p}$ (9 and 10

in Figure 3). In addition, the term $3a_1^4c_2$ corresponds to a type-V promolecules with the composition ABCXp$\bar{\text{p}}$, as depicted in Figure 5.

By the examination using the attached source code, the following equation is obtained as a net contribution of $a_1^4c_2$ to type V:

$$\begin{aligned} \mathrm{V}_2 = \frac{1}{48}(3(a_1^4c_2 - a_1^4c_2 + 2(a_4c_2 - a_2a_4) + 2(a_1^2a_2c_2 - a_1^2a_2^2) - 5(a_2^2c_2 - a_2^3) \\ - 8(a_1a_3c_2 - a_1a_3a_2) + 8(a_4c_2 - a_2a_4))) \end{aligned} \tag{35}$$

which leaves such necessary terms as $\mathrm{A^2BCp}\bar{\text{p}}$ (cf. Figure 3) and ABCXp$\bar{\text{p}}$ (cf. Figure 5). Note that the last line of Eq. 35 is added to omit such terms as $\mathrm{A^3Bp}\bar{\text{p}}$, which are shifted to contribute to the term $6\,a_1^2c_2^2$. As for octahedral stereoisomers with $\mathrm{A^2BCp}\bar{\text{p}}$, Figure 13 of [42].

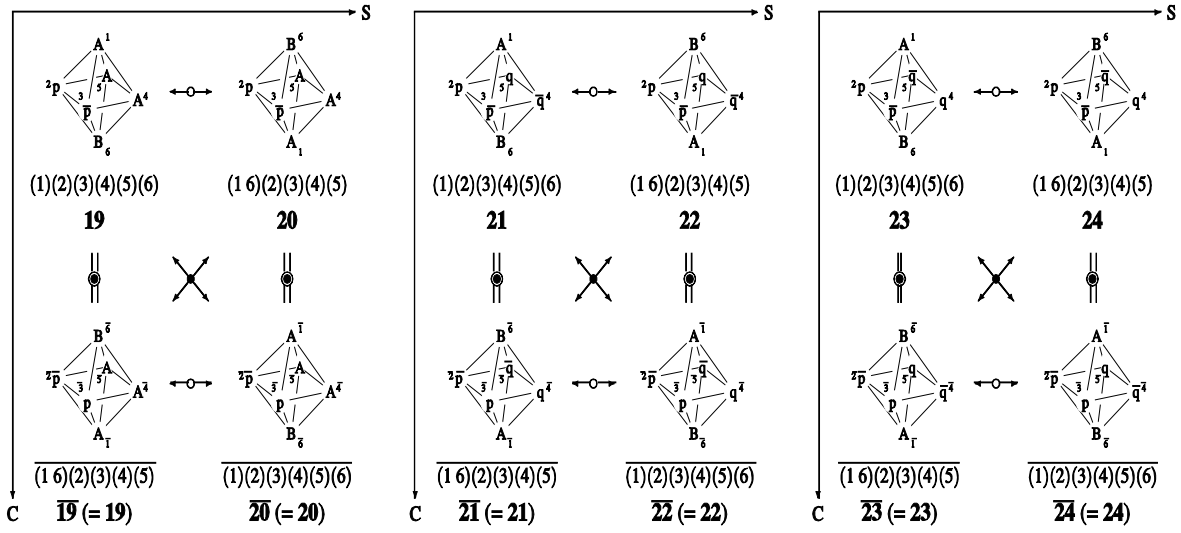

Figure 6. Type-V stereoisograms of promolecules with the compositions $\mathrm{A^3Bp}\bar{\text{p}}\,\text{p}$ and AB p$\bar{\text{p}}$q$\bar{\text{q}}$, which are evaluated by the PSI $a_1^2c_2^2$.

The term $6\,a_1^2c_2^2$ in Eq. 33 is concerned with the generation of such type-V promolecules as having the composition $\mathrm{A^3Bp}\bar{\text{p}}$ (the first stereoisogram in Figure 6) and AB p$\bar{\text{p}}$q$\bar{\text{q}}$ (the second and third stereoisograms in Figure 6)

By the examination using the attached source code, the following equation is obtained as a net contribution of $a_1^2c_2^2$ to type V:

$$\begin{aligned} V_3 = \frac{1}{48}(&6(a_1^2c_2^2 - 2(a_1^2c_4 - a_1^2a_4) - 2a_1^2a_2c_2 + a_1^2a_2^2 \\ &-(a_2c_2^2 - a_2^3) + 2(a_2c_4 - a_2a_4) + 2(a_2^2c_2 - a_2^3) \\ &+4(a_1a_3c_2 - a_1a_3a_2) - 4(a_4c_2 - a_2a_4))), \end{aligned} \tag{36}$$

which leaves such necessary terms as $A^3Bp\bar{p}$ and $ABp\bar{p}q\bar{q}$ (Figure 6). Note that the last line of Eq. 36 is added to take account of such terms as $A^3Bp\bar{p}$. The last line of Eq. 36 is cancelled be the last line of Eq. 35, when Eq. 35 and Eq. 36 are summed up.

Among the terms appearing in the right-hand side of Eq. 33, the terms $8c_6$ and $6c_2c_4$ do not contribute to the appearance of type-V stereoisograms. Hence, Eqs. 34, 35, and 36 are summed up to give the CI-CF for enumerating type-V stereoisograms:

$$\begin{aligned} \text{CI-CF}^{[V]}(O_{h\tilde{I}\hat{I}}) &= V_1+V_2+V_3 \\ &= -\frac{1}{16}a_1^4a_2 + \frac{1}{16}a_1^4c_2 - \frac{1}{8}a_1^2a_2c_2 + \frac{1}{8}a_1^2c_2^2 + \frac{1}{4}a_1^2a_4 - \frac{1}{4}a_1^2a_4 + \frac{1}{6}a_2^3 \\ &\quad -\frac{3}{16}a_2c_2^2 + \frac{1}{48}c_2^3 - \frac{1}{2}a_2a_4 + \frac{3}{8}a_2c_4 + \frac{1}{4}a_4c_2 - \frac{1}{8}c_2c_4 - \frac{1}{6}a_6 + \frac{1}{6}c_6. \end{aligned} \tag{37}$$

By introducing Eq. 37 into Eq. 33, the CI-CF for enumerating type-IV stereoisograms is obtained as follows:

$$\begin{aligned} \text{CI-CF}^{[IV]}(O_{h\tilde{I}\hat{I}}) &= \frac{1}{8}a_1^4a_2 + \frac{1}{4}a_1^2a_2c_2 - \frac{1}{2}a_1^2a_4 + \frac{1}{2}a_1^2c_4 - \frac{1}{3}a_2^3 \\ &\quad + \frac{3}{8}a_2c_2^2 + a_2a_4 - \frac{3}{4}a_2c_4 - \frac{1}{2}a_4c_2 + \frac{1}{2}c_2c_4 + \frac{1}{3}a_6. \end{aligned} \tag{38}$$

The modulated CI-CF is obtained by introducing Eq. 23 and Eq. 37 into Eq. 26:

$$\begin{aligned} \text{CI-CF}''(O_h) &= \text{CI-CF}(O_h) - \text{CI-CF}^{[V]}(O_{h\tilde{I}\hat{I}}) \\ &= \frac{1}{48}b_1^6 + \frac{1}{16}a_1^4a_2 + \frac{1}{16}b_1^2b_2^2 + \frac{1}{8}a_1^2a_2c_2 \\ &\quad + \frac{1}{8}b_1^2b_4 + \frac{1}{8}b_2^3 - \frac{1}{4}a_1^2a_4 + \frac{1}{4}a_1^2c_4 - \frac{1}{6}a_2^3 + \frac{3}{16}a_2c_2^2 + \frac{1}{6}b_3^2 \\ &\quad + \frac{1}{2}a_2a_4 - \frac{3}{8}a_2c_4 - \frac{1}{4}a_4c_2 + \frac{1}{4}c_2c_4 + \frac{1}{6}a_6. \end{aligned} \tag{39}$$

4.3. CI-CFs FOR ENUMERATING FIVE TYPES

Because the modulated CI-CF (Eq. 39 for CI-CF″(O_h)) has been obtained to revise the effect of CI-CF(O_h) (Eq. 9), it is used with the other CI-CFs, i.e., Eq. 17 for CI-CF(O), Eq. 18 for CI-CF($O_{\tilde{\imath}}$), Eq. 19 for CI-CF($O_{\hat{\imath}}$), and Eq. 20 for CI-CF($O_{h\tilde{\imath}\hat{\imath}}$). They are introduced into Eqs. 27–31. Thereby, we reach the following CI-CFs for enumerating stereoisograms of five types:

$$\begin{aligned}\text{CI-CF}^{[\text{I}]}(\text{O}_{h\tilde{\imath}\hat{\imath}}) = {} & \frac{1}{48}a_1^6 - \frac{1}{16}a_1^4a_2 - \frac{1}{8}a_1^2a_2c_2 + \frac{1}{16}a_1^2c_2^2 + \frac{1}{4}a_1^2a_4 - \frac{1}{8}a_1^2c_4 + \frac{1}{6}a_2^3 \\ & - \frac{3}{16}a_2c_2^2 + \frac{1}{8}c_2^3 - \frac{1}{2}a_2a_4 + \frac{3}{8}a_2c_4 + \frac{1}{6}a_3^2 + \frac{1}{4}a_4c_2 - \frac{1}{4}c_2c_4 - \frac{1}{6}a_6\end{aligned} \tag{40}$$

$$\begin{aligned}\text{CI-CF}^{[\text{II}]}(\text{O}_{h\tilde{\imath}\hat{\imath}}) = {} & \frac{1}{16}b_1^4b_2 - \frac{1}{16}a_1^4a_2 + \frac{1}{8}b_1^2b_2^2 - \frac{1}{8}a_1^2a_2c_2 + \frac{1}{48}b_2^3 + \frac{1}{4}a_1^2a_4 - \frac{1}{4}a_1^2c_4 + \frac{1}{6}a_2^3 \\ & - \frac{3}{16}a_2c_2^2 + \frac{1}{8}b_2b_4 - \frac{1}{2}a_2a_4 + \frac{3}{8}a_2c_4 + \frac{1}{4}a_4c_2 - \frac{1}{4}c_2c_4 + \frac{1}{6}b_6 - \frac{1}{6}a_6\end{aligned} \tag{41}$$

$$\begin{aligned}\text{CI-CF}^{[\text{III}]}(\text{O}_{h\tilde{\imath}\hat{\imath}}) = {} & \frac{1}{96}b_1^6 - \frac{1}{96}a_1^6 - \frac{1}{32}b_1^4b_2 + \frac{1}{16}a_1^4a_2 - \frac{1}{32}a_1^4c_2 - \frac{1}{32}b_1^2b_2^2 \\ & + \frac{1}{8}a_1^2a_2c_2 - \frac{3}{32}a_1^2c_2^2 + \frac{1}{16}b_1^2b_4 + \frac{5}{96}b_2^3 - \frac{1}{4}a_1^2a_4 + \frac{3}{16}a_1^2c_4 - \frac{1}{6}a_2^3 \\ & + \frac{3}{16}a_2c_2^2 - \frac{7}{96}c_2^3 - \frac{1}{16}b_2b_4 + \frac{1}{12}b_3^2 + \frac{1}{2}a_2a_4 - \frac{3}{8}a_2c_4 - \frac{1}{12}a_3^2 \\ & - \frac{1}{4}a_4c_2 + \frac{3}{16}c_2c_4 - \frac{1}{12}b_6 + \frac{1}{6}a_6 - \frac{1}{12}c_6\end{aligned} \tag{42}$$

$$\begin{aligned}\text{CI-CF}^{[\text{IV}]}(\text{O}_{h\tilde{\imath}\hat{\imath}}) = {} & \frac{1}{8}a_1^4a_2 + \frac{1}{4}a_1^2a_2c_2 - \frac{1}{2}a_1^2a_4 + \frac{1}{2}a_1^2c_4 - \frac{1}{3}a_2^3 \\ & + \frac{3}{8}a_2c_2^2 + a_2a_4 - \frac{3}{4}a_2c_4 - \frac{1}{2}a_4c_2 + \frac{1}{2}c_2c_4 + \frac{1}{3}a_6\end{aligned} \tag{43}$$

$$\begin{aligned}\text{CI-CF}^{[\text{V}]}(\text{O}_{h\tilde{\imath}\hat{\imath}}) = {} & -\frac{1}{16}a_1^4a_2 + \frac{1}{16}a_1^4c_2 - \frac{1}{8}a_1^2a_2c_2 + \frac{1}{8}a_1^2c_2^2 + \frac{1}{4}a_1^2a_4 - \frac{1}{4}a_1^2c_4 + \frac{1}{6}a_2^3 \\ & - \frac{3}{16}a_2c_2^2 + \frac{1}{48}c_2^3 - \frac{1}{2}a_2a_4 + \frac{3}{8}a_2c_4 + \frac{1}{4}a_4c_2 - \frac{1}{8}c_2c_4 - \frac{1}{6}a_6 + \frac{1}{6}c_6.\end{aligned} \tag{44}$$

The consistency of the modulated CI-CF (Eq. 39) is confirmed by the fact that Eq. 43 is identical with Eq. 38 and that Eq. 44 is identical with Eq. 37.

In order to conduct type-itemized enumeration of octahedral complexes, the ligand-inventory functions represented by Eqs. 11–13 are introduced into the type-itemized CI-CFs represented by Eqs. 40–44. The resulting equation of each type is expanded to give a generating function. In a similar way to the attached source code based on the GAP system, the full forms of Eqs. 11–13 are used in the type-itemized enumeration of this article. The number of inequivalent quadruplets of *RS*-stereoisomers (i.e., inequivalent stereoisograms) appears in the generating function as the coefficient of the term $A^aB^bC^cX^xY^yZ^zp^pp^pq^qq^qr^r\bar{r}^{\bar{r}}s^s\ \bar{s}^{\bar{S}}\ u^u\ \bar{u}^{\bar{u}}\ v^v\ \bar{v}^{\bar{v}}$, which is represented by the partition [θ] (Eq. 14).

Table 1. Type-Itemized Enumeration of Octahedral Complexes with Achiral Proligands.

partition for the composition $A^aB^bC^cX^xY^yZ^zp^pp^pq^qq^qr^r\bar{r}^{\bar{r}}s^s\ \bar{s}^{\bar{S}}\ u^u\bar{u}^{\bar{u}}\ v^v\bar{v}^{\bar{v}}$	gross O_h	enum. $O_{h\tilde{I}\hat{I}}$	type-itemized enum.				
			I	II	III	IV	V
$[\theta]_1$=[6,0,0,0,0,0,0,0,0,0,0,0,0,0,0,0,0,0]	1	1	0	0	0	1	0
$[\theta]_2$=[5,1,0,0,0,0,0,0,0,0,0,0,0,0,0,0,0,0]	1	1	0	0	0	1	0
$[\theta]_3$=[4,2,0,0,0,0,0,0,0,0,0,0,0,0,0,0,0,0]	2	2	0	0	0	2	0
$[\theta]_4$=[4,1,1,0,0,0,0,0,0,0,0,0,0,0,0,0,0,0]	2	2	0	0	0	2	0
$[\theta]_5$=[3,3,0,0,0,0,0,0,0,0,0,0,0,0,0,0,0,0]	2	2	0	0	0	2	0
$[\theta]_6$=[3,2,1,0,0,0,0,0,0,0,0,0,0,0,0,0,0,0]	3	3	0	0	0	3	0
$[\theta]_7$=[3,1,1,1,0,0,0,0,0,0,0,0,0,0,0,0,0,0]	4	4	1	0	0	3	0
$[\theta]_8$=[2,2,2,0,0,0,0,0,0,0,0,0,0,0,0,0,0,0]	5	5	1	0	0	4	0
$[\theta]_9$=[2,2,1,1,0,0,0,0,0,0,0,0,0,0,0,0,0,0]	6	6	2	0	0	4	0
$[\theta]_{10}$=[2,1,1,1,1,0,0,0,0,0,0,0,0,0,0,0,0,0]	9	9	6	0	0	3	0
$[\theta]_{11}$=[1,1,1,1,1,1,0,0,0,0,0,0,0,0,0,0,0,0]	15	15	15	0	0	0	0

5. ENUMERATION RESULTS

5.1. OCTAHEDRAL COMPLEXES WITH ACHIRAL PROLIGANDS ONLY

Table 1 collects type-itemized enumeration of octahedral complexes with achiral proligands only. The columns of gross enumeration indicate the numbers of octahedral complexes counted under the point group O_h and under the *RS*-stereoisomeric group $O_{h\tilde{I}\hat{I}}$. Note that a pair of (self)-enantiomers is counted once under the point group O_h, while a quadruplet of

RS-stereoisomers is counted once under the *RS*-stereoisomeric group $O_{h\tilde{I}\hat{I}}$. The columns of type-itemized enumeration (type I to type V) indicate the numbers of octahedral complexes of five types. The values of the gross enumeration under the point group O_h satisfy Eq. 23. The values of the gross enumeration under the *RS*-stereoisomeric group $O_{h\tilde{I}\hat{I}}$ satisfy Eq. 21.

Because Table 1 is concerned with achiral proligands only, there appear type-I or type-IV quadruplets. For example, the $[\theta]_7$-row of Table 1 indicates the presence of one type-I quadruplet and three type-IV quadruplets.

One type-I quadruplet with the composition A^3BCX ($[\theta]_7$) has been depicted in the type-I frame of Figure 3, which contains a pair of enantiomers $3/\overline{3}$. Note that a type-I quadruplet is generally characterized by the presence of diagonal equality symbols, so that it is chiral, *RS*-stereogenic, and ascleral (type index [−,−,*a*]).

The configuration of 3 (or $\overline{3}$) is specified by a configuration index *OC*-6-43 according tothe IUPAC rule IR-9.3.3.4 [43], where the priority sequence A > B > C > X is presumed. According to the IUPAC rule IR-9.3.4.8 [43], the absolute configuration of 3 is specified to be *OC*-6-23-*A*, while that of its *RS*-diastereomer 4 (=$\overline{3}$) is specified to be *OC*-6-43-*C*. Note that a pair of *C/A*-descriptors is assigned to a pair of *RS*-diastereomers (not to a pair of enantiomers) [33], strictly speaking, although a pair of *RS*-diastereomers is coincident with a pair of enantiomers in case of type-I stereoisograms.

Among the three type-IV quadruplets with the composition A^3BCX ($[\theta]_7$), one quadruplet has been depicted in the type-IV frame of Figure 3, which contains an achiral octahedral complex 8 having a *trans*-pair of proligands A–X. The remaining two type-IV quadruplets can be drawn by replacing the proligand X located at the *trans*-position of A by the proligand B or C so as to generate a *trans*-pair A–B or A–C. Note that a type-IV quadruplet is generally characterized by the presence of equality symbols in all directions, so that it is achiral, *RS*-astereogenic, and ascleral (type index [*a*,*a*,*a*]).

The three type-IV quadruplets are differentiated by configuration indices according to the IUPAC rule IR-9.3.3.4 [43]. The configuration index of 8 is determined to be *OC*-6-41, while the other two quadruplets are determined to be *OC*-6-21 and *OC*-6-31, respectively.

5.2. OCTAHEDRAL COMPLEXES WITH ACHIRAL AND CHIRAL PROLIGANDS

Table 2 collects type-itemized numbers of inequivalent quadruplets of *RS*-stereoisomers with achiral and chiral proligands. Each quadruplet of chiral promolecules is counted as a fractional value, as designated by an asterisk. For example, the value 1/2 at the intersection between the $[\theta]_{12}$-row (with an asterisk) and the type-II-column in Table 2 corresponds to such a term as $1\times\frac{1}{2}(A^5p+A^5\overline{p})$, which indicates the presence of one type-II quadruplet

of *RS*-stereoisomers. Note that the composition A^5p is converted into the composition $A^5\,\bar{p}$ vice versa under the action of a reflection. A type-II quadruplet is generally characterized by the presence of horizontal equality symbols, so that it is chiral, *RS*-astereogenic, and scleral (type index [−,*a*,−]).

The value 1 at the intersection between the $[\theta]_{13}$-row (with an asterisk) and the type-II column in Table 2 should be interpreted to correspond to such a term as $2\times1/2$ ($A^4p^2 + A^4\bar{p}^2$), which indicates the presence of two type-II quadruplets of *RS*-stereoisomers. Note that the composition A^4p^2 is converted into the composition $A^4\bar{p}^2$ vice versa under the action of a reflection. These type-II quadruplets are depicted in Figure 7. Each type-II quadruplet in Figure 7 contains a pair of enantiomers $25/2\bar{5}$ or $26/2\bar{6}$.

According to the IUPAC rule IR-9.3.3.4 [43], a configuration index *OC*-6-11 is assigned to 25 and $2\bar{5}$, where the priority sequence A > p or A > $\bar{p}$ is presumed. In a similar way, a configuration index *OC*-6-22 is assigned to 26 and $\overline{26}$. The absolute configuration for each pair of such enantiomers as belonging to type II is not specified by *C/A*-descriptors due to IUPAC rule IR-9.3.4.8, because of *RS*-astereogenicity (not because of achirality). For detailed discussions, see [33].

On the other hand, the value 2 at the intersection between the $[\theta]_{15}$-row (without an asterisk) and the type-IV-column in Table 2 should be interpreted to correspond to such a term as $2\times\ A^4p\,\bar{p}$, which indicates the presence of two type-IV quadruplets of *RS*-stereoisomers. Note that the composition $A^4p\,\bar{p}$ remains unchanged under the action of a reflection. These type-IV quadruplets are depicted in Figure 8.

The configurations of 27 and 28 can be differentiated by configuration indices according to the IUPAC rule IR-9.3.3.4 [43]. Thus, a configuration index *OC*-6-11 is assigned to 27, while a configuration index *OC*-6-32 is assigned to 28, where the priority sequence A > p > $\bar{p}$ is presumed.

The value 1 at the intersection between the $[\theta]_{19}$-row (without an asterisk) and the type-V column in Table 2 indicates the presence of one type-V quadruplet of *RS*-stereoisomers, which has the composition $A^3Bp\,\bar{p}$. The type-V quadruplet containing 19 and 20 has been drawn in Figure 6. According to the IUPAC rules IR-9.3.3.4 and IR-9.3.4.8 [43], 19 is determined to be *OC*-6-43-*a*, while 20 is determined to be *OC*-6-43-*c*, where the priority sequence A > B > p> $\bar{p}$ is presumed. Note that a pair of *C/A*-descriptors is assigned to a pair of *RS*-diastereomers 19/20, which is contained in a type-V stereoisogram shown in Figure 6. The chirality-unfaithful feature [11] is emphasized by the lowercase labels '*c/a*' used in place of the uppercase labels '*C/A*' [33].

The value 2 at the intersection between the $[\theta]_{29}$-row (with an asterisk) and the type-II column in Table 2 should be interpreted to correspond to such a term as $4\times1/2$ ($A^2BCp^2 + A^2BC\bar{p}^2$), which indicates the presence of four type-II quadruplets of *RS*-stereoisomers.

One type-II quadruplet containing $5/\overline{5}$ is drawn in Figure 3. The remaining three type-II quadruplets containing $29/\overline{29}$, $30/\overline{30}$, and $31/\overline{31}$ are depicted in Figure 9.

According to the IUPAC rule IR-9.3.3.4 [43], a configuration index *OC*-6-32 is assignedto 5 and $\overline{5}$, where the priority sequence A > B > C > p or A > B > C > $\overline{\text{p}}$ is presumed. In a similar way, a configuration index *OC*-6-14 is assigned to 29 and $\overline{29}$; a configuration index *OC*-6-13 is assigned to 30 and $\overline{30}$; and a configuration index *OC*-6-44 is assigned to 31 and $\overline{31}$. The absolute configuration for each pair of such enantiomers as belonging to type II is not specified by *C/A*-descriptors due to IUPAC rule IR-9.3.4.8, because of *RS*-astereogenicity (not because of achirality) [33].

Table 2. Type-Itemized Enumeration of Octahedral Complexes with Achiral and Chiral Proligands (Part 1).

partition for the composition	gross	enum.	type-itemized enum.				
$A^aB^bC^cX^xY^yZ^zp^pp^pq^qq^qr^r\bar{r}^{\bar{r}}s^s\bar{s}^{\bar{s}}u^u\bar{u}^{\bar{u}}v\bar{v}^{\bar{v}}$	O_h	$O_{h\tilde{I}\hat{I}}$	I	II	III	IV	V
$[\theta]^*_{12}$=[5,0,0,0,0,0,1,0,0,0,0,0,0,0,0,0,0,0]	1/2	1/2	0	1/2	0	0	0
$[\theta]^*_{13}$=[4,0,0,0,0,0,2,0,0,0,0,0,0,0,0,0,0,0]	1	1	0	1	0	0	0
$[\theta]^*_{14}$=[4,1,0,0,0,0,1,0,0,0,0,0,0,0,0,0,0,0]	1	1	0	1	0	0	0
$[\theta]^*_{15}$=[4,0,0,0,0,0,1,1,0,0,0,0,0,0,0,0,0,0]	2	2	0	0	0	2	0
$[\theta]^*_{16}$=[3,2,0,0,0,0,1,0,0,0,0,0,0,0,0,0,0,0]	3/2	3/2	0	3/2	0	0	0
$[\theta]^*_{17}$=[3,1,1,0,0,0,1,0,0,0,0,0,0,0,0,0,0,0]	5/2	2	0	3/2	1/2	0	0
$[\theta]^*_{18}$=[3,1,0,0,0,0,2,0,0,0,0,0,0,0,0,0,0,0]	3/2	3/2	0	3/2	0	0	0
$[\theta]^*_{19}$=[3,1,0,0,0,0,1,1,0,0,0,0,0,0,0,0,0,0]	4	3	0	2	1	0	0
$[\theta]^*_{20}$=[3,1,0,0,0,0,1,0,1,0,0,0,0,0,0,0,0,0]	5/2	2	0	3/2	1/2	0	0
$[\theta]^*_{21}$=[3,0,0,0,0,0,3,0,0,0,0,0,0,0,0,0,0,0]	1	1	0	1	0	0	0
$[\theta]^*_{22}$=[3,0,0,0,0,0,2,1,0,0,0,0,0,0,0,0,0,0]	3/2	3/2	0	3/2	0	0	0
$[\theta]^*_{23}$=[3,0,0,0,0,0,2,0,1,0,0,0,0,0,0,0,0,0]	3/2	3/2	0	3/2	0	0	0
$[\theta]^*_{24}$=[3,0,0,0,0,0,1,1,1,0,0,0,0,0,0,0,0,0]	5/2	2	0	3/2	1/2	0	0
$[\theta]^*_{25}$=[3,0,0,0,0,0,1,0,1,0,1,0,0,0,0,0,0,0]	5/2	2	0	3/2	1/2	0	0
$[\theta]^*_{26}$=[2,2,0,0,0,0,2,0,0,0,0,0,0,0,0,0,0,0]	3	5/2	0	2	1/2	0	0
$[\theta]^*_{27}$=[2,2,0,0,0,0,1,1,0,0,0,0,0,0,0,0,0,0]	6	5	0	0	1	4	0

$[\theta]^*_{28}$=[2,2,0,0,0,0,1,0,1,0,0,0,0,0,0,0,0,0]	4	3	0	2	1	0	0
$[\theta]^*_{29}$=[2,1,1,0,0,0,2,0,0,0,0,0,0,0,0,0,0,0]	4	3	0	2	1	0	0
$[\theta]^*_{30}$=[2,1,1,0,0,0,1,1,0,0,0,0,0,0,0,0,0,0]	10	6	0	1	2	1	2
$[\theta]^*_{31}$=[2,1,1,0,0,0,1,0,1,0,0,0,0,0,0,0,0,0]	15/2	9/2	0	3/2	3	0	0
$[\theta]^*_{32}$=[2,1,0,0,0,0,3,0,0,0,0,0,0,0,0,0,0,0]	3/2	3/2	0	3/2	0	0	0
$[\theta]^*_{33}$=[2,1,0,0,0,0,2,1,0,0,0,0,0,0,0,0,0,0]	4	3	0	2	1	0	0
$[\theta]^*_{34}$=[2,1,0,0,0,0,2,0,1,0,0,0,0,0,0,0,0,0]	4	3	0	2	1	0	0
$[\theta]^*_{35}$=[2,1,0,0,0,0,1,1,1,0,0,0,0,0,0,0,0,0]	15/2	9/2	0	3/2	3	0	0
$[\theta]^*_{36}$=[2,1,0,0,0,0,1,0,1,0,1,0,0,0,0,0,0,0]	15/2	9/2	0	3/2	3	0	0
$[\theta]^*_{37}$=[2,0,0,0,0,0,4,0,0,0,0,0,0,0,0,0,0,0]	1	1	0	1	0	0	0
$[\theta]^*_{38}$=[2,0,0,0,0,0,3,1,0,0,0,0,0,0,0,0,0,0]	3/2	3/2	0	3/2	0	0	0
$[\theta]^*_{39}$=[2,0,0,0,0,0,3,0,1,0,0,0,0,0,0,0,0,0]	3/2	3/2	0	3/2	0	0	0
$[\theta]^*_{40}$=[2,0,0,0,0,0,2,2,0,0,0,0,0,0,0,0,0,0]	4	4	1	1	0	2	0
$[\theta]^*_{41}$=[2,0,0,0,0,0,2,0,2,0,0,0,0,0,0,0,0,0]	3	5/2	0	2	1/2	0	0
$[\theta]^*_{42}$=[2,0,0,0,0,0,2,1,1,0,0,0,0,0,0,0,0,0]	4	3	0	2	1	0	0
$[\theta]^*_{43}$=[2,0,0,0,0,0,2,0,1,1,0,0,0,0,0,0,0,0]	4	3	0	2	1	0	0
$[\theta]^*_{44}$=[2,0,0,0,0,0,2,0,1,0,1,0,0,0,0,0,0,0]	4	3	0	2	1	0	0
$[\theta]^*_{45}$=[2,0,0,0,0,0,1,1,1,1,0,0,0,0,0,0,0,0]	9	7	2	0	2	3	0
$[\theta]^*_{46}$=[2,0,0,0,0,0,1,1,1,0,1,0,0,0,0,0,0,0]	15/2	9/2	0	3/2	3	0	0
$[\theta]^*_{47}$=[2,0,0,0,0,0,1,0,1,0,1,0,1,0,0,0,0,0]	15/2	9/2	0	3/2	3	0	0

The value 1 at the intersection between The $[\theta]_{29}$-row (with an asterisk) and the type-III column in Table 2 should be interpreted to correspond to such a term as $2 \times 1/2$ ($A^2BCp^2 + A^2BC\,\bar{p}^{\,2}$), which indicates the presence of two type-III quadruplets of *RS*-stereoisomers. They are depicted in Figure 10. A type-III quadruplet is generally characterized by the absence of equality symbols in all directions, so that it is chiral, *RS*-stereogenic, and scleral (type index [−,−,−]).

The $[\theta]_{30}$-row (without an asterisk) in Table 2 indicates the presence of one type-II, two type-III, one type-IV, and two type-V stereoisograms.

One type-II quadruplet of *RS*-stereoisomers $36/\overline{36}$ with the composition $A^2BCp\,\bar{p}$ is depicted in the upperleft part of Figure 11. According to the IUPAC rule IR-9.3.3.4 [43], a

configuration index *OC*-6-15 is assigned to 36, while *OC*-6-14 is assigned to 36, where the priority sequence A > B > C > p > $\overline{p}$ is presumed. The absolute configuration for each pair of such enantiomers as belonging to type II is not specified by *C/A*-descriptors due to IUPAC rule IR-9.3.4.8, because of *RS*-astereogenicity (not because of achirality) [33].

Among the two type-III quadruplets with $A^2BCp\,\overline{p}$ ($[\theta]_{30}$), one has been already depicted in the type-III frame of Figure 3 ($6/\overline{6}/7/\overline{7}$). The other is depicted in the upperright part of Figure 11 ($37/\overline{37}/38/\overline{38}$). As for the type-III frame of Figure 3, *OC*-6-52-*C* assigned to 6 is paired with *OC*-6-52-*A* assigned to 7, while *OC*-6-42-*A* assigned to 6 is paired with *OC*-6-42-*C* assigned to 7. As for the upperright part of Figure 11, *OC*-6-53-*C* assigned to 37 is paired with *OC*- 6-53-*A* assigned to 38, while *OC*-6-43-*A* assigned to 37 is paired with *OC*-6-43-*C* assigned to $\overline{38}$. It should be noted that *OC*-6-52-*C* assigned to 6 , for example, is not paired with *OC*-6-42-*A* assigned to $\overline{6}$, because the configuration-index parts are different from each other, even though the *C/A*-labels are paired. It follows that a pair of *C/A*-descriptors is assigned to a pair of *RS*-diastereomers, not to a pair of enantiomers.

One type-IV quadruplet, which consists of an achiral promolecule 39 with the composition $A^2BCp\,\overline{p}$, is depicted in the lower left part of Figure 11.

Among the two type-V quadruplets with the composition $A^2BCp\,\overline{p}$, one has been depicted in the type-V frame of Figure 3 (9/10). The other is depicted in the lowerright part of Figure 11 (40/41). The pair of 9/10 (or the pair of 40/41) is in an *RS*-diastereomeric relationship, which is specified by *C/A*-descriptors due to IUPAC rule IR-9.3.4.8. When the priority sequence A > B > C > p > $\overline{p}$ is presumed, *OC*-6-32-*a* assigned to 9 is paired with *OC*-6-32-*c* assigned to 10; and *OC*-6-54-*a* assigned to 40 is paired with *OC*-6-54-*c* assigned to 41. The lowercase labels *c/a* are used to emphasize the chirality-unfaithful features of type-V quadruplets.

Table 3 is the list of additional type-itemized numbers of inequivalent quadruplets of *RS*-stereoisomers with achiral and chiral proligands.

The $[\theta]_{49}$-row (without an asterisk) in Table 3 indicates the presence of six type-III and three type-V stereoisograms. The three type-V quadruplets with the composition ABCXp $\overline{p}$ have been already depicted in Figure 5, where each type-V quadruplet is characterized to be achiral, *RS*-stereogenic, and scleral (type index [*a*,–,–]). The pair of 13/14 (or 15/16 or 17/18) exhibits an *RS*-diastereomeric relationship, which corresponds to the term 'pseudoasymmetry' in the conventional terminology of stereochemistry. When the priority sequence A > B > C > X > p > $\overline{p}$ is presumed, *OC*-6-43-*a* assigned to 13 is paired with *OC*-6-43-*c* assigned to 14; *OC*-6-24-*c* assigned to 15 is paired with *OC*-6-24-*a* assigned to 16; and *OC*-6-34-*a* assigned to 17 is paired with *OC*-6-34-*c* assigned to 18.

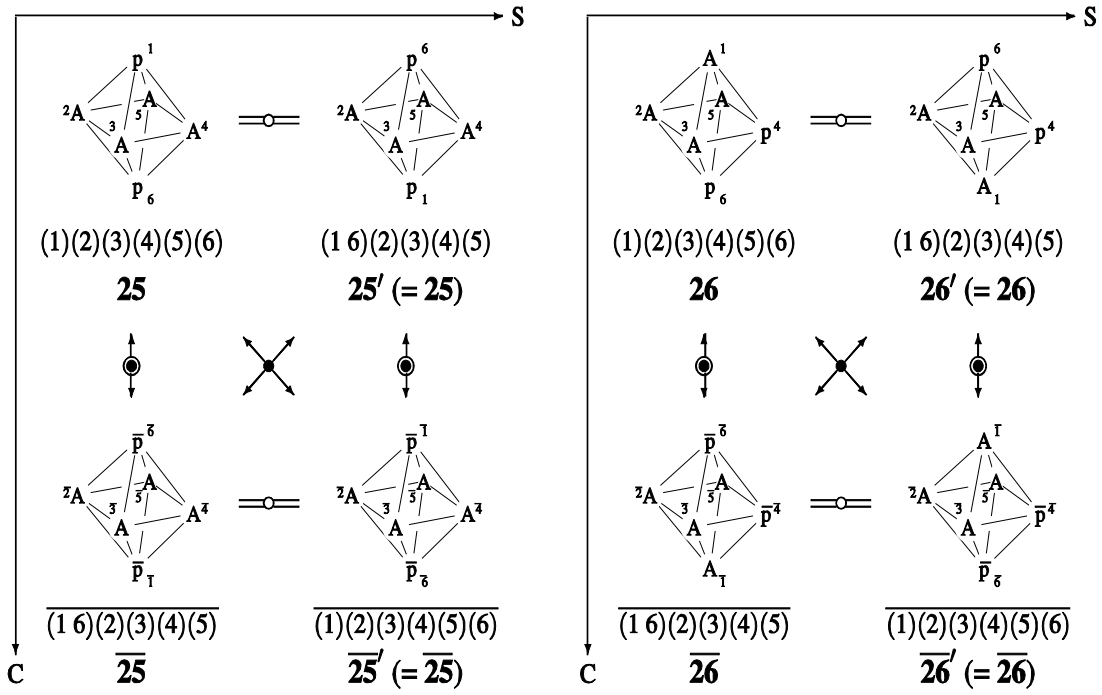

Figure 7. Type-II stereoisograms of promolecules with the composition 1/2 ($A^4p^2+A^4\bar{p}^2$), which corresponds to the $[\theta]_{13}$-row of Table 2.

The $[\theta]_{62}$-row (without an asterisk) in Table 3 indicates the presence of one type-I, six type-III, and two type-V stereoisograms. The two type-V quadruplets with the composition $ABp\bar{p}q\bar{q}$ ($[\theta]_{62}$) have been already depicted in Figure 6, where each type-V quadruplet is characterized to be achiral, *RS*-stereogenic, and scleral (type index [*a*,−,−]). The pair of 21/22 (or 23/24) exhibits an *RS*-diastereomeric relationship, which corresponds to the term 'pseudoasymmetry' in the conventional terminology of stereochemistry. When the priority sequence A > B > p > $\bar{p}$ > q > $\bar{q}$ is presumed, *OC*-6-26-*a* assigned to 21 is paired with *OC*-6-26-*c* assigned to 22; and *OC*-6-25-*a* assigned to 23 is paired with *OC*-6-25-*c* assigned to 24.

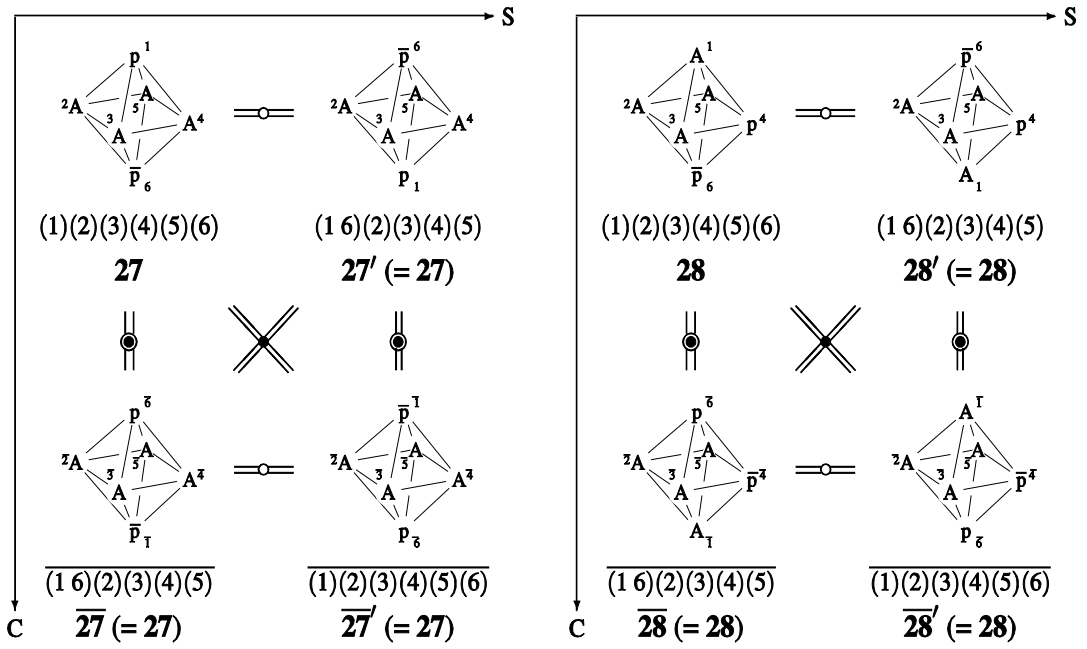

Figure 8. Type-IV stereoisograms of promolecules with the composition $A^4p\,\bar{p}$, which corresponds to the $[\theta]_{15}$-row of Table 2.

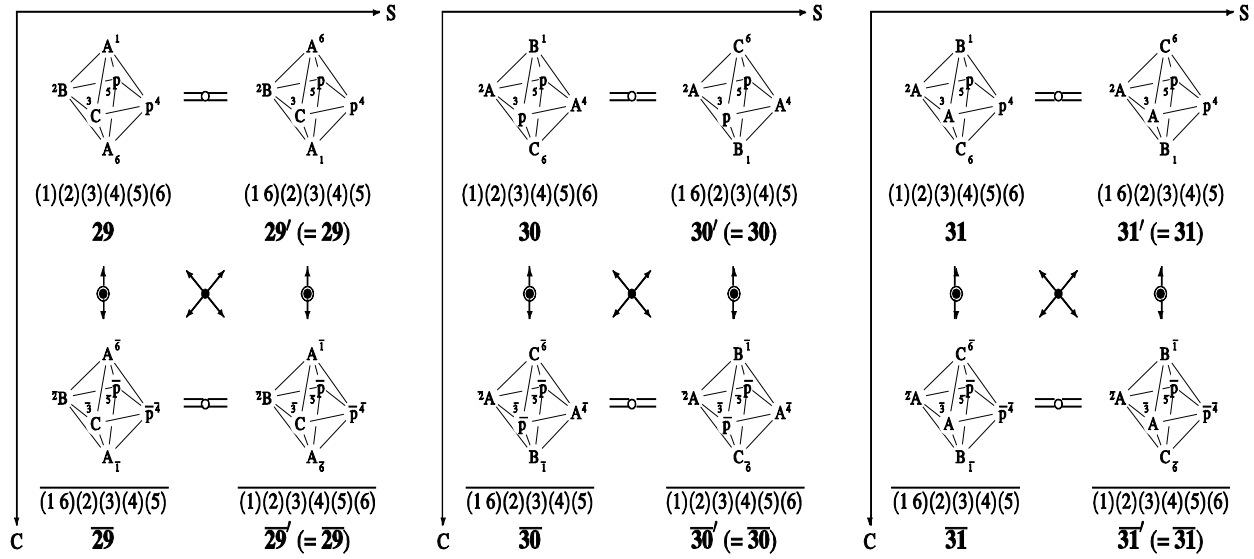

Figure 9. Type-II stereoisograms of promolecules with the composition $1/2(A^2BCp^2+A^2BC\,\bar{p}^{\,2})$, which corresponds to the $[\theta]_{29}$-row of Table 2. One more type-II stereoisogram $(5/\bar{5})$ is drawn in Figure 3.

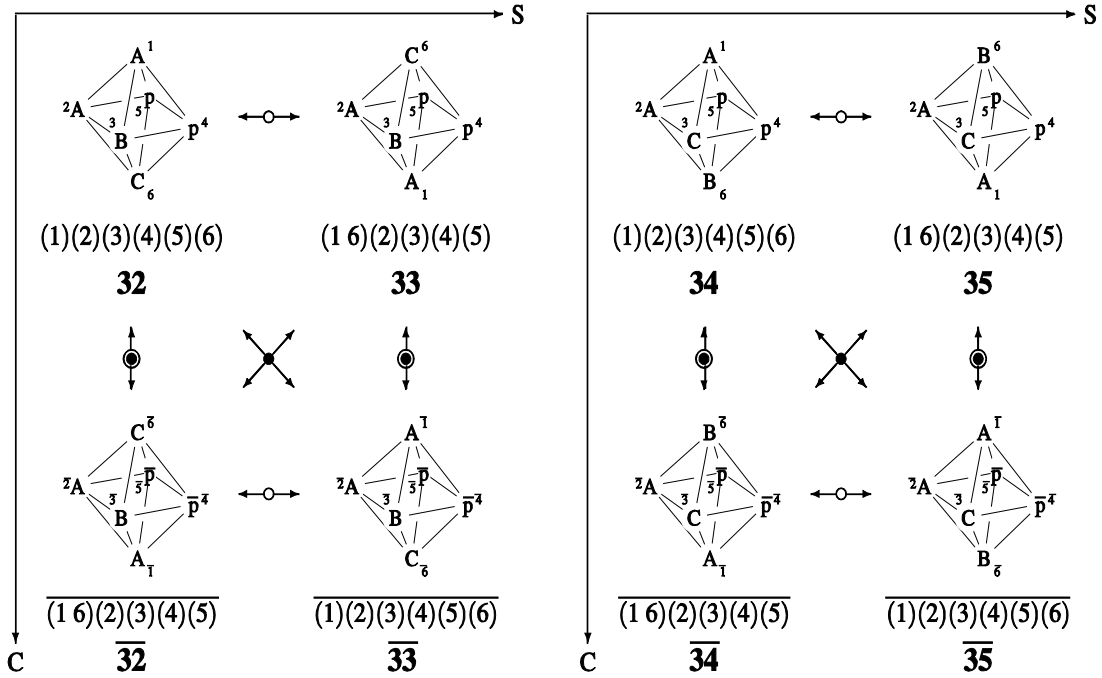

Figure 10. Type-III stereoisograms of promolecules with the composition 1/2 (A^2BCp^2 + $A^2BC\,\overline{p}^{\,2}$), which corresponds to the $[\theta]_{29}$-row of Table 2.

The type-I quadruplet with the composition $ABp\,\overline{p}\,q\,\overline{q}$ ($[\theta]_{62}$) is depicted in Figure 12. The chiral, *RS*-stereogenic, and ascleral behavior of Figure 12 (type index [−,−,*a*]) is characterized by the presence of equality symbols in the diagonal directions, so that the *RS*-diastereomeric relationship between 42 and 43 (= $\overline{42}$) is coincident with the enantiomeric relationship between 42 and $\overline{42}$. When the priority sequence A > B > p > $\overline{p}$ > q > $\overline{p}$ is presumed, *OC*-6-24- *A* assigned to 42 is paired with *OC*-6-24-*C* assigned to 43. The pair of the labels assigned originally to a pair of *RS*-diastereomers 42/43 can be interpreted to be assigned to a pair of enantiomers 42/ $\overline{42}$ (= 43) in a chirality-faithful fashion [11].

5.3. OCTAHEDRAL COMPLEXES WITH CHIRAL PROLIGANDS ONLY

Table 4 collects type-itemized numbers of inequivalent quadruplets of *RS*-stereoisomers with chiral proligands only.

The value of 1 at the intersection between the $[\theta]_{111}$-row and the type-V-column in Table 4 indicates the presence of one type-V stereoisogram with the composition $p\,\overline{p}\,q\,\overline{q}\,r\,\overline{r}$. The type-V stereoisogram has been depicted in Figure 4, in which a pair of 11 and 12 is

determined to be *RS*-diastereomeric. When the priority sequence $p > \bar{p} > q > \bar{q} > r > \bar{r}$ is presumed, *OC*-6-24-*a* assigned to 11 is paired with *OC*-6-24-*c* assigned to 12.

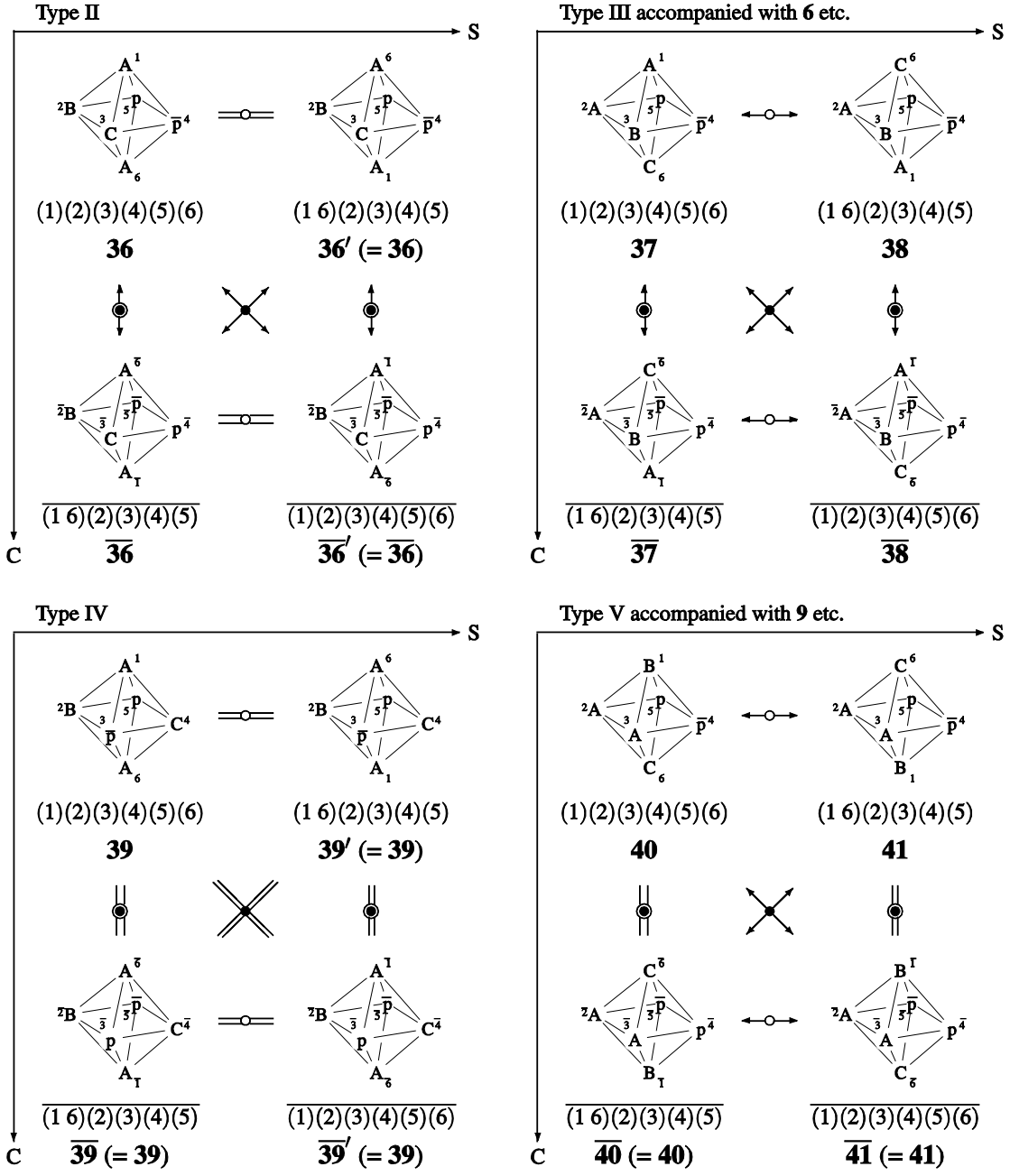

Figure 11. Several stereoisograms of promolecules with the composition $A^2BCp\,\bar{p}$, which corresponds to the $[\theta]_{30}$-row of Table 2.

6. CONCLUSION

Fujita's proligand method [28] is extended to treat type-itemized enumeration of quadruplets of octahedral complexes under the action of the corresponding *RS*-stereoisomeric group. A modulated CI-CF is evaluated from the CI-CF of the point group O_h by trial-and error calculation of type-V quadruplets contained in stereoisograms. Then, the modulated CI-CF is combined with a CI-CF of the maximum chiral point group (O), a CI-CF of the maximum *RS*-permutation group, a CI-CF of the maximum ligand-reflection group, and a CI-CF of the *RS*-stereoisomeric group so as to generate CI-CFs for evaluating type-I to type-V quadruplets. By introducing ligand-inventory functions into the CI-CFs, the numbers of quadruplets of octahedral complexes are obtained and shown in tabular forms. Several stereoisograms for typical complexes are depicted. Their configuration indices due to IUPAC rule IR-9.3.3.4 [43] as well as *C/A* descriptors due to IUPAC rule IR-9.3.4.8 are discussed on the basis of Fujita's stereoisogram approach [34].

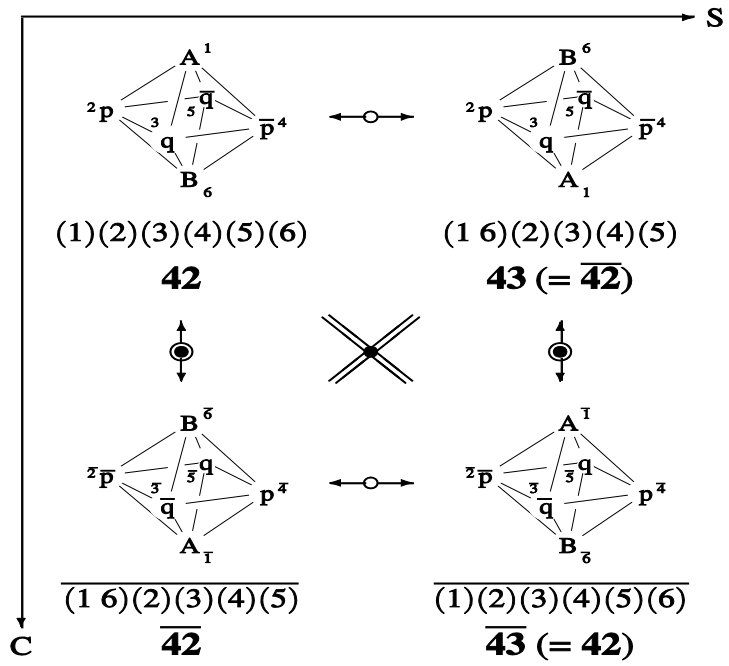

Figure 12. Type-I stereoisogram of promolecules with the composition $ABp\,\bar{p}\,q\,\bar{q}$, which corresponds to the $[\theta]_{62}$-row of Table 3.

APPENDIX

The following source code for evaluation of the modulated CI-CF is based on the GAP system [44]. The file named test_V.gap containing this code is stored in a directory shown in the command Read. This Read sentence is copied and pasted on a command line of the

GAP system. The execution result is stored in the log file named test_Vlog.txt, which is specified by the command LogTo. The type-itemized enumeration can be done by using the CI-CFs of the respective types (Eqs. 40–44) in place of V_1 etc.

```
#Read("c:/fujita0/fujita2015/ligancy6/calcGAP/test_V.gap");
LogTo("c:/fujita0/fujita2015/ligancy6/calcGAP/test_Vlog.txt");
#####################
# Setting variables #
#####################
A := Indeterminate(Rationals, "A"); B := Indeterminate(Rationals, "B");
C := Indeterminate(Rationals, "C"); x := Indeterminate(Rationals, "x");
y := Indeterminate(Rationals, "y"); z := Indeterminate(Rationals, "z");
p := Indeterminate(Rationals, "p"); P := Indeterminate(Rationals, "P");
q := Indeterminate(Rationals, "q"); Q := Indeterminate(Rationals, "Q");
r := Indeterminate(Rationals, "r"); R := Indeterminate(Rationals, "R");
s := Indeterminate(Rationals, "s"); S := Indeterminate(Rationals, "S");
u := Indeterminate(Rationals, "u"); U := Indeterminate(Rationals, "U");
v := Indeterminate(Rationals, "v"); V := Indeterminate(Rationals, "V");
b_1 := Indeterminate(Rationals, "b_1"); b_2 := Indeterminate(Rationals, "b_2");
b_3 := Indeterminate(Rationals, "b_3"); b_4 := Indeterminate(Rationals, "b_4");
b_5 := Indeterminate(Rationals, "b_5"); b_6 := Indeterminate(Rationals, "b_6");
a_1 := Indeterminate(Rationals, "a_1"); a_2 := Indeterminate(Rationals, "a_2");
a_3 := Indeterminate(Rationals, "a_3"); a_4 := Indeterminate(Rationals, "a_4");
a_5 := Indeterminate(Rationals, "a_5"); a_6 := Indeterminate(Rationals, "a_6");
c_2 := Indeterminate(Rationals, "c_2"); c_4 := Indeterminate(Rationals, "c_4");
c_6 := Indeterminate(Rationals, "c_6");
####################
#type IV + 2 type V#
####################
CICF_VI_V := (1/24)*(c_2^3 + 3*a_1^4*c_2 + 8*c_6 + 6*a_1^2*c_2^2 + 6*c_2*c_4);
##############################
#Evaluation of the term c_2^3#
##############################
V1 := (1/48)*(c_2^3 - 3*(a_2*c_2^2 - a_2^2*c_2) - 6*(c_2*c_4 - a_2*c_4 - a_4*c_2
+ a_2*a_4) + 8*(c_6 - a_6) - a_2^3);
##################################
#Evaluation of the term a_1^4*c_2#
##################################
V2 := (1/48)*(3*(a_1^4*c_2 - a_1^4*a_2 + 2*(a_4*c_2 - a_2*a_4)
```

```
+ 2*(a_1^2*a_2*c_2 - a_1^2*a_2^2) - 5*(a_2^2*c_2 - a_2^3)
- 8*(a_1*a_3*c_2-a_1*a_3*a_2) + 8*(a_4*c_2 - a_2*a_4)));
####################################
#Evaluation of the term a_1^2*c_2^2#
####################################
V3 := (1/48)*(6*(a_1^2*c_2^2 - 2*(a_1^2*c_4 - a_1^2*a_4) - 2*a_1^2*a_2*c_2
+ a_1^2*a_2^2 - (a_2*c_2^2 - a_2^3) + 2*(a_2*c_4 - a_2*a_4) + 2*(a_2^2*c_2 - a_2^3)
+ 4*(a_1*a_3*c_2-a_1*a_3*a_2) - 4*(a_4*c_2 - a_2*a_4)));
##################
# CI-CF of type V#
##################
CICF_V := V1 + V2 + V3;
##################
# CI-CF of type IV#
##################
CICF_IV := CICF_VI_V - 2*CICF_V;
############################
#Ligand-inventory functions#
############################
aa_1 := A + B + C + x;
aa_2 := A^2 + B^2 + C^2 + x^2;
aa_3 := A^3 + B^3 + C^3 + x^3;
aa_4 := A^4 + B^4 + C^4 + x^4;
aa_6 := A^6 + B^6 + C^6 + x^6;
bb_3 := A^3 + B^3 + C^3 + x^3 + p^3 + P^3 + q^3 + Q^3 + r^3 + R^3;
bb_4 := A^4 + B^4 + C^4 + x^4 + p^4 + P^4 + q^4 + Q^4 + r^4 + R^4;
bb_6 := A^6 + B^6 + C^6 + x^6 + p^6 + P^6 + q^6 + Q^6 + r^6 + R^6;
cc_2 := A^2 + B^2 + C^2 + x^2 + 2*p*P + 2*q*Q + 2*r*R;
cc_4 := A^4 + B^4 + C^4 + x^4 + 2*p^2*P^2 + 2*q^2*Q^2 + 2*r^2*R^2;
cc_6 := A^6 + B^6 + C^6 + x^6 + 2*p^3*P^3 + 2*q^3*Q^3 + 2*r^3*R^3;
######################
#Generating functions#
######################
Display("##### CICF_VI_V, f_CICF_VI_V --- type IV + 2 type V ######");
Print("CICF_VI_V := ", CICF_VI_V, "\n");
f_CICF_VI_V:= Value(CICF_VI_V,
[a_1, a_2, a_3, a_4, a_6, b_1, b_2, b_3, b_4, b_6, c_2, c_4, c_6],
[aa_1, aa_2, aa_3, aa_4, aa_6, bb_1, bb_2, bb_3, bb_4, bb_6, cc_2, cc_4, cc_6]);
Print("f_CICF_VI_V := ", f_CICF_VI_V, "\n");
```

```
Display("##### V1, f_V1 --- term c_2^3 ######");
Print("V1 := ", V1, "\n");
f_V1:= Value(V1,
[a_1, a_2, a_3, a_4, a_6, b_1, b_2, b_3, b_4, b_6, c_2, c_4, c_6],
[aa_1, aa_2, aa_3, aa_4, aa_6, bb_1, bb_2, bb_3, bb_4, bb_6, cc_2, cc_4, cc_6]);
Print("f_V1 := ", f_V1, "\n");
Display("##### V2, f_V2 --- term a_1^4*c_2 ######");
Print("V2 := ", V2, "\n");
f_V2:= Value(V2,
[a_1, a_2, a_3, a_4, a_6, b_1, b_2, b_3, b_4, b_6, c_2, c_4, c_6],
[aa_1, aa_2, aa_3, aa_4, aa_6, bb_1, bb_2, bb_3, bb_4, bb_6, cc_2, cc_4, cc_6]);
Print("f_V2 := ", f_V2, "\n");
Display("##### V3, f_V3 --- term a_1^2*c_2^2 ######");
Print("V3 := ", V3, "\n");
f_V3:= Value(V3,
[a_1, a_2, a_3, a_4, a_6, b_1, b_2, b_3, b_4, b_6, c_2, c_4, c_6],
[aa_1, aa_2, aa_3, aa_4, aa_6, bb_1, bb_2, bb_3, bb_4, bb_6, cc_2, cc_4, cc_6]);
Print("f_V3 := ", f_V3, "\n");
Display("##### CICF_V, f_CICF_V --- type V ######");
Print("CICF_V := ", CICF_V, "\n");
f_CICF_V:= Value(CICF_V,
[a_1, a_2, a_3, a_4, a_6, b_1, b_2, b_3, b_4, b_6, c_2, c_4, c_6],
[aa_1, aa_2, aa_3, aa_4, aa_6, bb_1, bb_2, bb_3, bb_4, bb_6, cc_2, cc_4, cc_6]);
Print("f_CICF_V := ", f_CICF_V, "\n");
Display("##### CICF_IV, f_CICF_IV --- type IV ######");
Print("CICF_IV := ", CICF_IV, "\n");
f_CICF_IV:= Value(CICF_IV,
[a_1, a_2, a_3, a_4, a_6, b_1, b_2, b_3, b_4, b_6, c_2, c_4, c_6],
[aa_1, aa_2, aa_3, aa_4, aa_6, bb_1, bb_2, bb_3, bb_4, bb_6, cc_2, cc_4, cc_6]);
Print("f_CICF_IV := ", f_CICF_IV, "\n");
LogTo();
```

Table 3. Type-Itemized Enumeration of Octahedral Complexes with Achiral and Chiral Proligands (Part 2).

partition for the composition $A^aB^bC^cX^xY^yZ^zp^pp^pq^qq^qr^r\bar{r}^{\bar{r}}s^s\bar{s}^{\bar{s}}u^u\bar{u}^{\bar{u}}v\bar{v}^{\bar{v}}$	gross O_h	enum. $O_{h\tilde{I}\hat{I}}$	type-itemized enum.				
			I	II	III	IV	V
$[\theta]^*_{48}$ = [1,1,1,1,1,0,1,0,0,0,0,0,0,0,0,0,0,0]	15	15/2	0	0	15/2	0	0
$[\theta]^*_{49}$ = [1,1,1,1,0,0,1,1,0,0,0,0,0,0,0,0,0,0]	18	9	0	0	6	0	3
$[\theta]^*_{50}$ = [1,1,1,1,0,0,1,0,1,0,0,0,0,0,0,0,0,0]	15	15/2	0	0	15/2	0	0
$[\theta]^*_{51}$ = [1,1,1,0,0,0,3,0,0,0,0,0,0,0,0,0,0,0]	5/2	2	0	3/2	1/2	0	0
$[\theta]^*_{52}$ = [1,1,1,0,0,0,2,1,0,0,0,0,0,0,0,0,0,0]	15/2	9/2	0	3/2	3	0	0
$[\theta]^*_{53}$ = [1,1,1,0,0,0,2,0,1,0,0,0,0,0,0,0,0,0]	15/2	9/2	0	3/2	3	0	0
$[\theta]^*_{54}$ = [1,1,1,0,0,0,1,1,1,0,0,0,0,0,0,0,0,0]	15	15/2	0	0	15/2	0	0
$[\theta]^*_{55}$ = [1,1,0,0,0,0,4,0,0,0,0,0,0,0,0,0,0,0]	1	1	0	1	0	0	0
$[\theta]^*_{56}$ = [1,1,0,0,0,0,3,1,0,0,0,0,0,0,0,0,0,0]	5/2	2	0	3/2	1/2	0	0
$[\theta]^*_{57}$ = [1,1,0,0,0,0,3,0,1,0,0,0,0,0,0,0,0,0]	5/2	2	0	3/2	1/2	0	0
$[\theta]^*_{58}$ = [1,1,0,0,0,0,2,2,0,0,0,0,0,0,0,0,0,0]	5	4	0	1	1	2	0
$[\theta]^*_{59}$ = [1,1,0,0,0,0,2,1,1,0,0,0,0,0,0,0,0,0]	15/2	9/2	0	3/2	3	0	0
$[\theta]^*_{60}$ = [1,1,0,0,0,0,2,0,1,1,0,0,0,0,0,0,0,0]	15/2	9/2	0	3/2	3	0	0
$[\theta]^*_{61}$ = [1,1,0,0,0,0,2,0,1,0,1,0,0,0,0,0,0,0]	15/2	9/2	0	3/2	3	0	0
$[\theta]^*_{62}$ = [1,1,0,0,0,0,1,1,1,1,0,0,0,0,0,0,0,0]	17	9	1	0	6	0	2
$[\theta]^*_{63}$ = [1,1,0,0,0,0,1,1,1,0,1,0,0,0,0,0,0,0]	15	15/2	0	0	15/2	0	0
$[\theta]^*_{64}$ = [1,1,0,0,0,0,1,0,1,0,1,0,1,0,0,0,0,0]	15	15/2	0	0	15/2	0	0
$[\theta]^*_{65}$ = [1,0,0,0,0,0,5,0,0,0,0,0,0,0,0,0,0,0]	1/2	1/2	0	1/2	0	0	0
$[\theta]^*_{66}$ =[1,0,0,0,0,0,4,1,0,0,0,0,0,0,0,0,0,0]	1	1	0	1	0	0	0
$[\theta]^*_{67}$ =[1,0,0,0,0,0,4,0,1,0,0,0,0,0,0,0,0,0]	1	1	0	1	0	0	0
$[\theta]^*_{68}$ =[1,0,0,0,0,0,3,2,0,0,0,0,0,0,0,0,0,0]	3/2	3/2	0	3/2	0	0	0
$[\theta]^*_{69}$ =[1,0,0,0,0,0,3,0,2,0,0,0,0,0,0,0,0,0]	3/2	3/2	0	3/2	0	0	0
$[\theta]^*_{70}$ =[1,0,0,0,0,0,3,1,1,0,0,0,0,0,0,0,0,0]	5/2	2	0	3/2	1/2	0	0
$[\theta]^*_{71}$ =[1,0,0,0,0,0,3,0,1,1,0,0,0,0,0,0,0,0]	5/2	2	0	3/2	1/2	0	0

$[\theta]^{*}_{72}$ =[1,0,0,0,0,0,3,0,1,0,1,0,0,0,0,0,0,0]	5/2	2	0	3/2	1/2	0	0
$[\theta]^{*}_{73}$ =[1,0,0,0,0,0,2,2,1,0,0,0,0,0,0,0,0,0]	4	3	0	2	1	0	0
$[\theta]^{*}_{74}$ = [1,0,0,0,0,0,2,1,2,0,0,0,0,0,0,0,0,0]	4	3	0	2	1	0	0
$[\theta]^{*}_{75}$ =[1,0,0,0,0,0,2,1,1,1,0,0,0,0,0,0,0,0]	15/2	9/2	0	3/2	3	0	0
$[\theta]^{*}_{76}$ =[1,0,0,0,0,0,2,1,1,0,1,0,0,0,0,0,0,0]	15/2	9/2	0	3/2	3	0	0
$[\theta]^{*}_{77}$ =[1,0,0,0,0,0,2,0,1,1,1,0,0,0,0,0,0,0]	15/2	9/2	0	3/2	3	0	0
$[\theta]^{*}_{78}$ =[1,0,0,0,0,0,2,0,1,0,1,0,1,0,0,0,0,0]	15/2	9/2	0	3/2	3	0	0
$[\theta]^{*}_{79}$ =[1,0,0,0,0,0,1,1,1,1,1,0,0,0,0,0,0,0]	15	15/2	0	0	15/2	0	0
$[\theta]^{*}_{80}$ =[1,0,0,0,0,0,1,1,1,0,1,0,1,0,0,0,0,0]	15	15/2	0	0	15/2	0	0
$[\theta]^{*}_{81}$ =[1,0,0,0,0,0,1,0,1,0,1,0,1,0,1,0,0,0]	15	15/2	0	0	15/2	0	0

Table 4. Type-Itemized Enumeration of Octahedral Complexes with Chiral Proligands.

partition for the composition $A^{a}B^{b}C^{c}X^{x}Y^{y}Z^{z}p^{p}p^{p}q^{q}q^{q}r^{r}\bar{r}^{\bar{r}}s^{s}\bar{s}^{\bar{s}}u^{u}\bar{u}^{\bar{u}}v\bar{v}^{\bar{v}}$	gross O_h	enum. $O_{h\tilde{I}\hat{I}}$	type-itemized enum.				
			I	II	III	IV	V
$[\theta]^{*}_{82}$ =[0,0,0,0,0,0,6,0,0,0,0,0,0,0,0,0,0,0]	1/2	1/2	0	1/2	0	0	0
$[\theta]^{*}_{83}$ =[0,0,0,0,0,0,5,1,0,0,0,0,0,0,0,0,0,0]	1/2	1/2	0	1/2	0	0	0
$[\theta]^{*}_{84}$ =[0,0,0,0,0,0,5,0,1,0,0,0,0,0,0,0,0,0]	1/2	1/2	0	1/2	0	0	0
$[\theta]^{*}_{85}$ =[0,0,0,0,0,0,4,2,0,0,0,0,0,0,0,0,0,0]	1	1	0	1	0	0	0
$[\theta]^{*}_{86}$ =[0,0,0,0,0,0,4,0,2,0,0,0,0,0,0,0,0,0]	1	1	0	1	0	0	0
$[\theta]^{*}_{87}$ =[0,0,0,0,0,0,4,1,1,0,0,0,0,0,0,0,0,0]	1	1	0	1	0	0	0
$[\theta]^{*}_{88}$ =[0,0,0,0,0,0,4,0,1,1,0,0,0,0,0,0,0,0]	1	1	0	1	0	0	0
$[\theta]^{*}_{89}$ =[0,0,0,0,0,0,4,0,1,0,1,0,0,0,0,0,0,0]	1	1	0	1	0	0	0
$[\theta]^{*}_{90}$ =[0,0,0,0,0,0,3,3,0,0,0,0,0,0,0,0,0,0]	2	2	0	0	0	2	0
$[\theta]^{*}_{91}$ =[0,0,0,0,0,0,3,0,3,0,0,0,0,0,0,0,0,0]	1	1	0	1	0	0	0
$[\theta]^{*}_{92}$ =[0,0,0,0,0,0,3,2,1,0,0,0,0,0,0,0,0,0]	3/2	3/2	0	3/2	0	0	0
$[\theta]^{*}_{93}$ =[0,0,0,0,0,0,3,1,2,0,0,0,0,0,0,0,0,0]	3/2	3/2	0	3/2	0	0	0
$[\theta]^{*}_{94}$ =[0,0,0,0,0,0,3,1,1,1,0,0,0,0,0,0,0,0]	5/2	2	0	3/2	1/2	0	0
$[\theta]^{*}_{95}$ =[0,0,0,0,0,0,3,1,1,0,1,0,0,0,0,0,0,0]	5/2	2	0	3/2	1/2	0	0

$[\theta]^*_{96}$ =[0,0,0,0,0,0,3,0,2,1,0,0,0,0,0,0,0,0]	3/2	3/2	0	3/2	0	0	0
$[\theta]^*_{97}$ =[0,0,0,0,0,0,3,0,2,0,1,0,0,0,0,0,0,0]	3/2	3/2	0	3/2	0	0	0
$[\theta]^*_{98}$ =[0,0,0,0,0,0,3,0,1,1,1,0,0,0,0,0,0,0]	5/2	2	0	3/2	1/2	0	0
$[\theta]^*_{99}$ =[0,0,0,0,0,0,3,0,1,0,1,0,1,0,0,0,0,0]	5/2	2	0	3/2	1/2	0	0
$[\theta]^*_{100}$ =[0,0,0,0,0,0,2,2,2,0,0,0,0,0,0,0,0,0]	3	5/2	0	2	1/2	0	0
$[\theta]^*_{101}$ =[0,0,0,0,0,0,2,2,1,1,0,0,0,0,0,0,0,0]	5	5	2	1	0	2	0
$[\theta]^*_{102}$ =[0,0,0,0,0,0,2,2,1,0,1,0,0,0,0,0,0,0]	4	3	0	2	1	0	0
$[\theta]^*_{103}$ =[0,0,0,0,0,0,2,1,2,1,0,0,0,0,0,0,0,0]	4	3	0	2	1	0	0
$[\theta]^*_{104}$ =[0,0,0,0,0,0,2,1,2,0,1,0,0,0,0,0,0,0]	4	3	0	2	1	0	0
$[\theta]^*_{105}$ =[0,0,0,0,0,0,2,1,1,1,1,0,0,0,0,0,0,0]	15/2	9/2	0	3/2	3	0	0
$[\theta]^*_{106}$ =[0,0,0,0,0,0,2,1,1,0,1,0,1,0,0,0,0,0]	15/2	9/2	0	3/2	3	0	0
$[\theta]^*_{107}$ =[0,0,0,0,0,0,2,0,2,0,2,0,0,0,0,0,0,0]	3	5/2	0	2	1/2	0	0
$[\theta]^*_{108}$ =[0,0,0,0,0,0,2,0,2,0,1,1,0,0,0,0,0,0]	4	3	0	2	1	0	0
$[\theta]^*_{109}$ =[0,0,0,0,0,0,2,0,1,1,1,1,0,0,0,0,0,0]	15/2	9/2	0	3/2	3	0	0
$[\theta]^*_{110}$ =[0,0,0,0,0,0,2,0,1,1,1,0,1,0,0,0,0,0]	15/2	9/2	0	3/2	3	0	0
$[\theta]^*_{111}$ =[0,0,0,0,0,0,1,1,1,1,1,1,0,0,0,0,0,0]	16	11	6	0	4	0	1
$[\theta]^*_{112}$ =[0,0,0,0,0,0,1,1,1,1,1,0,1,0,0,0,0,0]	15	15/2	0	0	15/2	0	0
$[\theta]^*_{113}$ =[0,0,0,0,0,0,1,1,1,0,1,0,1,0,1,0,0,0]	15	15/2	0	0	15/2	0	0
$[\theta]^*_{114}$ =[0,0,0,0,0,0,1,0,1,0,1,0,1,0,1,0,1,0]	15	15/2	0	0	15/2	0	0

REFERENCES

1. S. Fujita, Integrated discussion on stereogenicity and chirality for restructuring stereochemistry, *J. Math. Chem.* **35** (2004) 265–287.
2. S. Fujita, A proof for the existence of five stereogenicity types on the basis of the existence of five types of subgroups of *RS*-stereoisomeric groups. Hierarchy of groups for restructuring stereochemistry (Part 3), *MATCH Commun. Math. Comput. Chem.* **54** (2005) 39–52.

3. S. Fujita, Stereogenicity revisited. Proposal of holantimers for comprehending the relationship between stereogenicity and chirality, *J. Org. Chem.* **69** (2004) 3158–3165.
4. S.Fujita, Pseudoasymmetry, stereogenicity, and the *RS*-nomenclature comprehended by the concepts of holantimers and stereoisograms, *Tetrahedron* **60** (2004) 11629–11638.
5. S. Fujita, Stereoisograms for discussing chirality and stereogenicity of allene derivatives, *Memoirs of the Faculty of Engineering and Design, Kyoto Institute of Technology* **53** (2005) 19–38.
6. J. A. Le Bel, Sur les relations qui existent entre les formules atomiques des corps organique et le pouvoir rotatoire de leurs dissolutions, *Bull. Soc. Chim. Fr. (2)* **22** (1874) 337–347.
7. J. A. Le Bel, On the Relations Which Exist Between the Atomic Formulas of Organic Compounds and the Rotatory Power of Their Solutions, In *Classics in the Theory of Chemical Combination (Classics of Science, Vol. I)*; O. T. Benfey, Ed., Dover: New York, 1963; pp 161–171.
8. J. H. van't Hoff, Voorstel tot Uitbreiding der tegenwoordig in de scheikunde gebruikte Structure-Formules in de ruimte; benevens een daarmee samenhangende opmerking omtrent het verband tusschen optisch Vermogen en Chemische Constitutie van Organische Verbindingen, *Archives N´eerlandaises des Sciences exactes et naturelles* **9** (1874) 445–454.
9. J. H. van't Hoff, A Suggestion Looking to the Extension into Space of the Structural Formulas at Present Used in Chemistry. And a Note Upon the Relation Between the Optical Activity and the Chemical Constitution of Organic Compounds, In *Foundations of Stereochemistry, Memoirs of Pasteur, van't Hoff, Le Bel and Wislicenus*; G. M. Richardson, Ed., American Book Co.: New York, 1901; pp 35–46.
10. S. Fujita, Stereoisograms for specifying chirality and *RS*-stereogenicity. A versatile tool for avoiding the apparent inconsistency between geometrical features and *RS*--nomenclature in stereochemistry, *MATCH Commun. Math. Comput. Chem.* **61** (2009) 11– 38.
11. S. Fujita, *RS*-Stereodescriptors determined by *RS*-stereogenicity and their chiralityfaithfulness, *J. Comput. Aided Chem.* **10** (2009) 16–29.
12. S. Fujita, Complete settlement of long-standing confusion on the term "prochirality" in stereochemistry. Proposal of pro-*RS*-stereogenicity and integrated treatment with prochirality, *Tetrahedron* **62** (2006) 691–705.
13. S. Fujita, Substitution criteria based on stereoisograms to determine prochirality and pro-*RS*-stereogenicity, *MATCH Commun. Math. Comput. Chem.* **61** (2009) 39–70.

14. S. Fujita, *Pro-R/pro-S*-Descriptors specified by *RS*-diastereotopic relationships, not by stereoheterotopic relationships, *J. Comput. Aided Chem.* **10** (2009) 76–95.
15. S. Fujita, Stereoisograms for reorganizing the theoretical foundations of stereochemistry and stereoisomerism: I. Diagrammatic representations of *RS*-stereoisomeric groups for integrating point groups and *RS*-permutation groups, *Tetrahedron: Asymmetry* **25** (2014) 1153–1168.
16. S. Fujita, Stereoisograms for reorganizing the theoretical foundations of stereochemistry and stereoisomerism: II. Rational avoidance of misleading standpoints for *R/S*stereodescriptors of the Cahn-Ingold-Prelog system, *Tetrahedron: Asymmetry* **25** (2014) 1169–1189.
17. S. Fujita, Stereoisograms for reorganizing the theoretical foundations of stereochemistry and stereoisomerism: III. Rational avoidance of misleading standpoints for *Pro-R/Pro-S*descriptors, *Tetrahedron: Asymmetry* **25** (2014) 1190–1204.
18. S. Fujita, The stereoisogram approach for remedying discontents of stereochemical terminology, *Tetrahedron: Asymmetry* **25** (2014) 1612–1623.
19. S. Fujita, *Symmetry and Combinatorial Enumeration in Chemistry*, Springer-Verlag, Berlin-Heidelberg, 1991.
20. S. Fujita, *Diagrammatical Approach to Molecular Symmetry and Enumeration of Stereoisomers*, University of Kragujevac, Faculty of Science, Kragujevac, 2007.
21. S. Fujita, Symmetry-itemized enumeration of quadruplets of *RS*-stereoisomers: I — The fixed-point matrix method of the USCI approach combined with the stereoisogram approach, *J. Math. Chem.* **52** (2014) 508–542.
22. S. Fujita, Symmetry-itemized enumeration of quadruplets of *RS*-stereoisomers: II — The partial-cycle-index method of the USCI approach combined with the stereoisogram approach, *J. Math. Chem.* **52** (2014) 543–574.
23. S. Fujita, Symmetry-itemized enumeration of *RS*-stereoisomers of allenes. I. The fixedpoint matrix method of the USCI approach combined with the stereoisogram approach, *J. Math. Chem.* **52** (2014) 1717–1750.
24. S. Fujita, Symmetry-itemized enumeration of *RS*-stereoisomers of allenes. II. The partialcycle- index method of the USCI approach combined with the stereoisogram approach, *J. Math. Chem.* **52** (2014) 1751–1793.
25. S. Fujita, Stereoisograms for three-membered heterocycles: I. Symmetry-itemized enumeration of oxiranes under an *RS*-stereoisomeric group, *J. Math. Chem.* **53** (2015) 260–304.
26. S. Fujita, Stereoisograms for three-membered heterocycles: II. Chirality, *RS*-stereogenicity, and ortho-stereogenicity on the basis of the proligand-promolecule model, *J. Math. Chem.* **53** (2015) 305–352.

27. S. Fujita, Stereoisograms for three-membered heterocycles: III. *R/S*-stereodescriptors for characterizing the *RS*-stereogenic aspect of absolute configuration, *J. Math. Chem.* **53** (2015) 353–373.
28. S. Fujita, *Combinatorial Enumeration of Graphs, Three-Dimensional Structures, and Chemical Compounds*, University of Kragujevac, Faculty of Science, Kragujevac, 2013.
29. S. Fujita, Combinatorial enumeration of *RS*-stereoisomers itemized by chirality, *RS*-stereogenicity, and sclerality, *MATCH Commun. Math. Comput. Chem.* **58** (2007) 611– 634.
30. S. Fujita, Itemized enumeration of quadruplets of *RS*-stereoisomers under the action of *RS*-stereoisomeric groups, *MATCH Commun. Math. Comput. Chem.* **61** (2009) 71–115.
31. S. Fujita, Type-itemized enumeration of quadruplets of *RS*-stereoisomers. I. Cycle indices with chirality fittingness modulated by type-IV quadruplets, *J. Math. Chem.* (2015); DOI 10.1007/s10910-015-0561-z.
32. S. Fujita, Type-itemized enumeration of quadruplets of *RS*-stereoisomers: II. Cycle indices with chirality fittingness modulated by type-V quadruplets, *J. Math. Chem.* (2015); DOI 10.1007/s10910-015-0562-y.
33. S. Fujita, Stereoisograms of octahedral complexes. I. Chirality and *RS*-stereogenicity, *MATCH Commun. Math. Comput. Chem.* **71** (2014) 511–536.
34. S. Fujita, *Mathematical Stereochemistry*, De Gruyter, Berlin, 2015.
35. S. Fujita, Promolecules with a subsymmetry of O_h. Combinatorial enumeration and stereochemical properties, *Polyhedron* **12** (1993) 95–110.
36. S. Fujita, Symmetry-itemized enumeration of cubane derivatives as three-dimensional entities by the fixed-point matrix method of the USCI approach, *Bull. Chem. Soc. Jpn.* **84** (2011) 1192–1207.
37. S. Fujita, Generalization of partial cycle indices and modified bisected mark tables for combinatorial enumeration, *Bull. Chem. Soc. Jpn.* **73** (2000) 329–339.
38. S. Fujita, Graphs to chemical structures 1. Sphericity indices of cycles for stereochemical extension of Pólya's theorem, *Theor. Chem. Acc.* **113** (2005) 73–79.
39. S. Fujita, Graphs to chemical structures 2. Extended sphericity indices of cycles for stereochemical extension of Pólya's coronas, *Theor. Chem. Acc.* **113** (2005) 80–86.
40. S. Fujita, Graphs to chemical structures 3. General theorems with the use of different sets of sphericity indices for combinatorial enumeration of nonrigid stereoisomers, *Theor. Chem. Acc.* **115** (2006) 37–53.
41. S. Fujita, Stereochemistry and stereoisomerism characterized by the sphericity concept, *Bull. Chem. Soc. Jpn.* **74** (2001) 1585–1603.

42. S. Fujita, Stereoisograms of octahedral complexes. II. *RS*-Stereogenicity vs. stereogenicity as well as *RS*-stereoisomerism vs. stereoisomerism, *MATCH Commun. Math. Comput. Chem.* **71** (2014) 537–574.
43. N. G. Connelly, T. Damhus, R. M. Hartshorn, A. T. Hutton, and IUPAC, *Nomenclature of Inorganic Chemistry*, *IUPAC Recommendations 2005*, RSC Publishing, Cambridge, 2005.
44. The GAP Team, GAP – Groups, Algorithms and Programming, version 4.4.10, 2010, http://www.gap-system.org.